高温超伝導の数値的研究

T. Yanagisawa[1], M. Miyazaki[2], S. Koikegami[3] and K. Yamaji[1]

[1]National Institute of Advanced Industrial Science and Technology (AIST), Nanoelectronics Research Institute
[2]Aoyama Gakuin University
[3]Second Lab.

Contents

1. Introduction

Key words: Physics from U (Coulomb interactions)

- A possibility of superconductivity
  - Superconductivity from U
- Competition of AF and SC
- Incommensurate state
  - Stripes and SC
  - Compete and Collaborate
- Stripes in the lightly-doped region
- Singular Spectral function

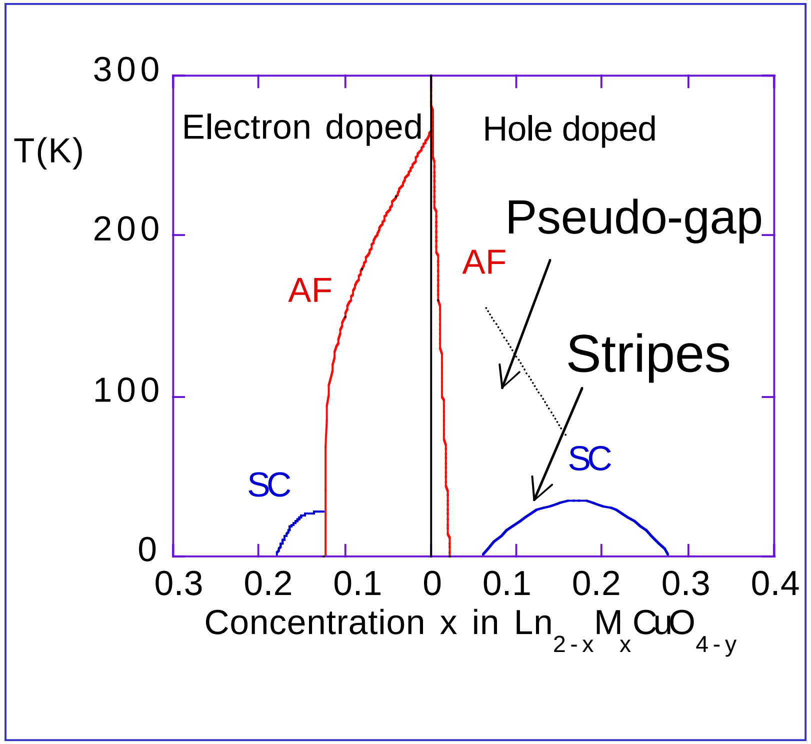

Purpose of Theoretical study

1. Origin of the superconductivity
   - Symmetry of Cooper pairs
   - Mechanism of attractive interaction

     Coulomb interaction U, Exchange interaction J

2. Physics of Anomalous Metallic behavior
   - Inhomogeneous electronic states: stripe
   - Pseudogap phenomena
   - Structural transition LTO, LTT

2. Superconductivity

1911 カマリン·オネス

電気抵抗

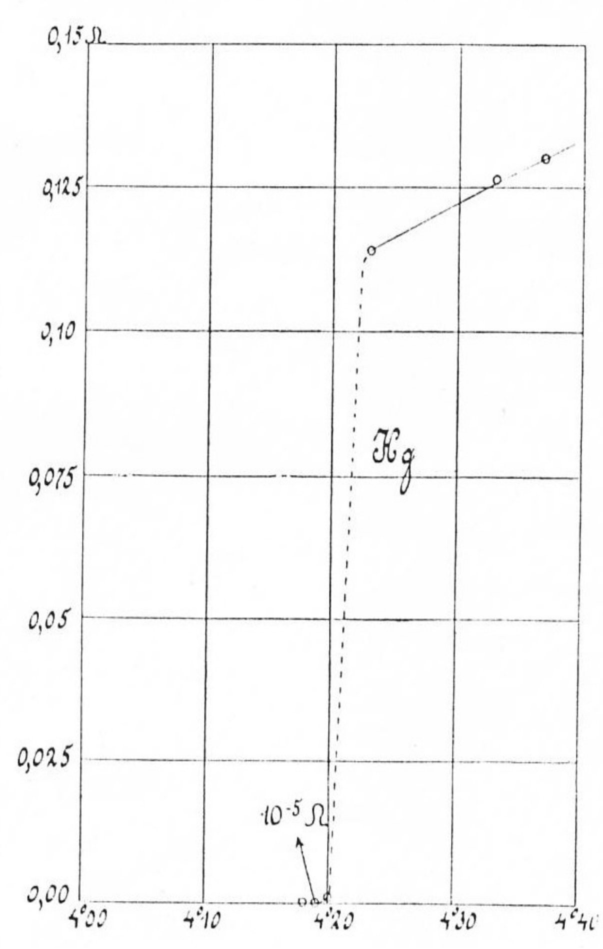

絶対温度 K

超伝導になる元素

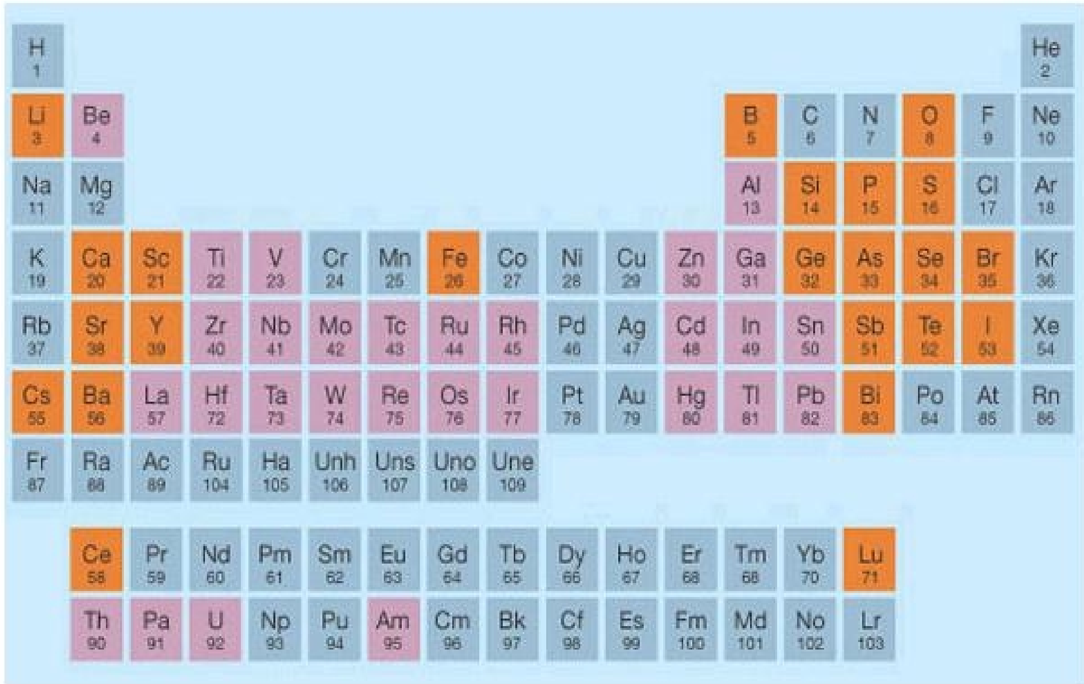

Y. Maeno

冷やすと超伝導になる

圧力をかけると初めて超伝導になる

巨視的量子現象

kと-kの電子がペアーをつくり、ゲージ（位相）不変性が破れた状態

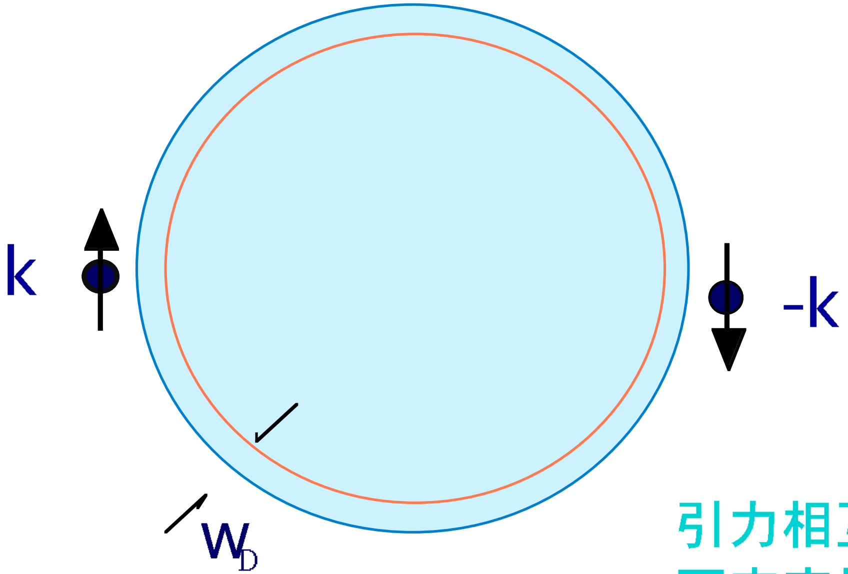

BCS理論

電子には位相という仮想的空間内での回転の自由度があり、勝手な方向を向いている。が、超伝導状態ではすべての電子ペアが同じ方向を向いている。

対称性の破れ

引力相互作用によるフェルミ面の不安定性によって超伝導がひきおこされる

超伝導体の特徴

電気抵抗 0

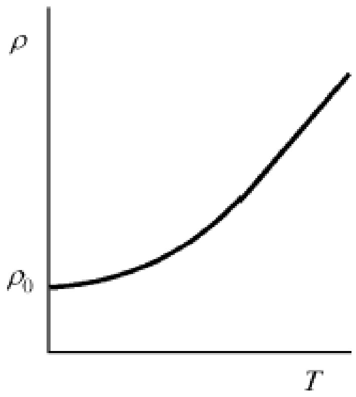

金属

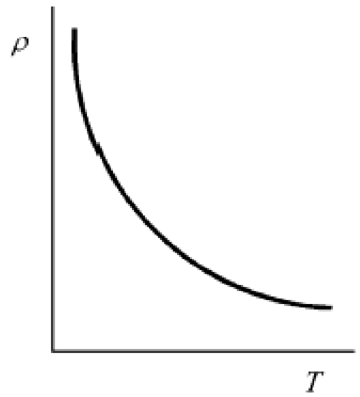

半導体

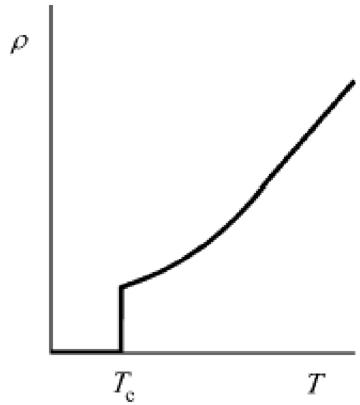

超伝導体

マイスナー効果

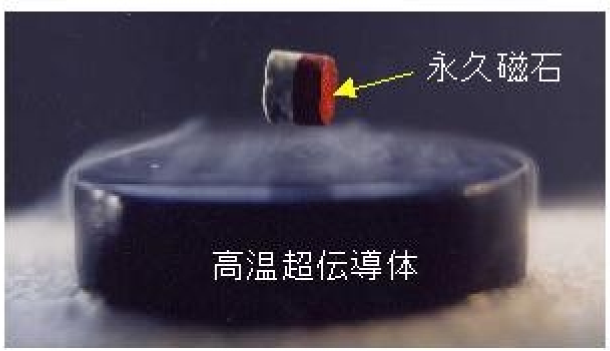

磁場は超伝導体に入り込むことができない

フッシング効果　超伝導体に磁石を近付けておいて冷やすと超伝導体内部に入り込んだ磁場により（第２種超伝導体）、つりあげることができる。

超伝導

（近藤淳「超伝導」（固体物理）より）

BCS理論　どうして電子対を考えたか

超伝導状態：　一つのSlater行列式では表わせない

電子間引力　H_1

$$H = H_0 + H_1 \qquad \Psi = \sum_j c_j \Psi_j$$

Ψ_j : Slater行列式

Ψ_0 : Fermi球

波動関数　$\Psi = c_0 \Psi + \sum_{j \neq 0} c_j \Psi_j$　　摂動計算　$c_0 \approx 1$

$$c_j \left\langle \Psi_0 H_1 \Psi_j \right\rangle < 0$$

エネルギー　$\left\langle \Psi H \Psi \right\rangle = \sum c_j^2 \left\langle \Psi_j H_0 \Psi_j \right\rangle + \sum c_i c_j \left\langle \Psi_i H_1 \Psi_j \right\rangle$

もし、すべての $\left\langle \Psi_i H_1 \Psi_j \right\rangle < 0$ なら、すべての $c_j > 0$

Ψ_jとしてペアーの状態をとるならば、$c_j>0$として
エネルギーを下げることができる。

超伝導（２）

電子対

$$\Psi_i = \left| k_1 \uparrow -k_1 \downarrow, k_2 \uparrow -k_2 \downarrow, k_3 \uparrow -k_3 \downarrow, \cdots \right\rangle$$

$$\Psi_j = \left| k'_1 \uparrow - k'_1 \downarrow, k_2 \uparrow -k_2 \downarrow, k_3 \uparrow -k_3 \downarrow, \cdots \right\rangle$$

順番を変えても
符号は変わらない。

$$\left\langle \Psi_i H_1 \Psi_j \right\rangle = \left\langle k'_1 - k'_1 \middle| V \middle| k_1 - k_1 \right\rangle < 0$$

非対角要素を常に負にできる

基底状態はすべての対状態の一次結合で表わされる:

$$\Psi = \sum c_{k_1 k_2 \cdots} \left| k_1 \uparrow -k_1 \downarrow, k_2 \uparrow -k_2 \downarrow, \cdots \right\rangle$$

独立対近似（一体近似）をすると

$$\Psi = \sum c_{k_1} c_{k_2} \cdots \left| k_1 \uparrow -k_1 \downarrow, k_2 \uparrow -k_2 \downarrow, \cdots \right\rangle$$

N電子項のみを取り出すとして

$$\Phi = \prod_k \left(u_k + v_k \left| k \uparrow -k \downarrow \right\rangle \right)$$

BCSの波動関数

$$\frac{\sqrt{\left(N - \langle N \rangle\right)^2}}{\langle N \rangle} \propto \frac{1}{\sqrt{\langle N \rangle}}$$

粒子数のゆらぎは小さい

3. 高温超伝導

超伝導臨界温度

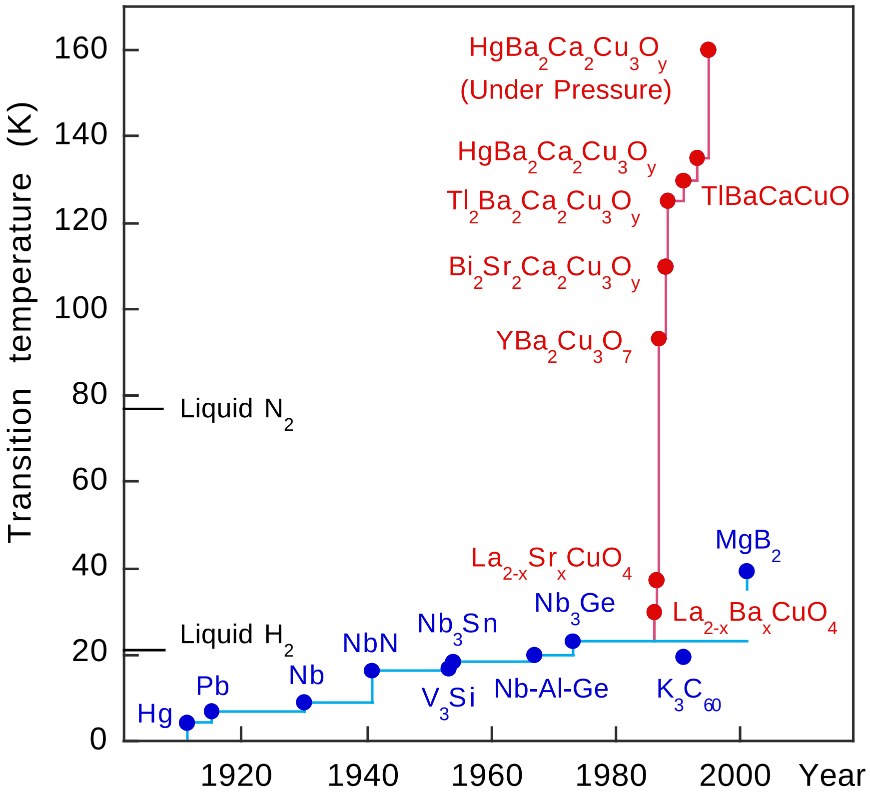

ペルブスカイト　銅酸化物

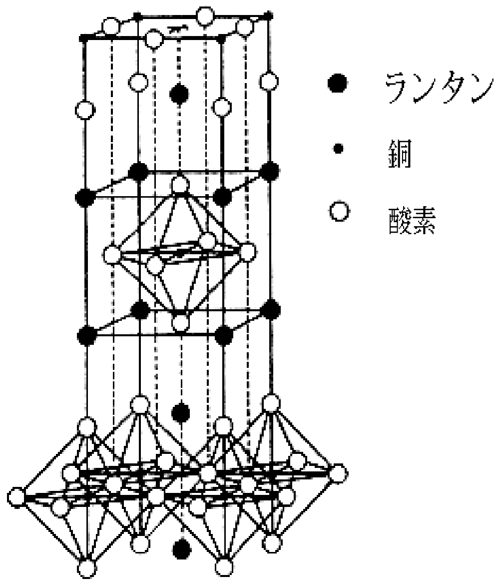

LaSrCuO

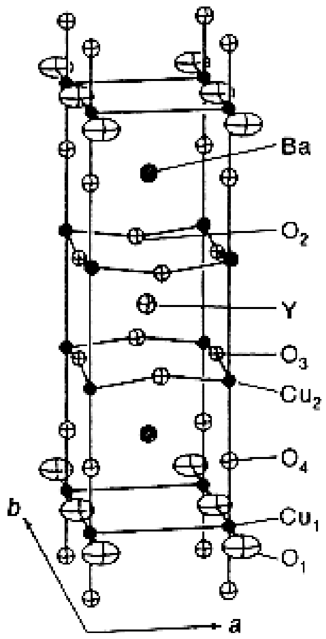

YBaCuO

高温超伝導の相図

Phase diagram

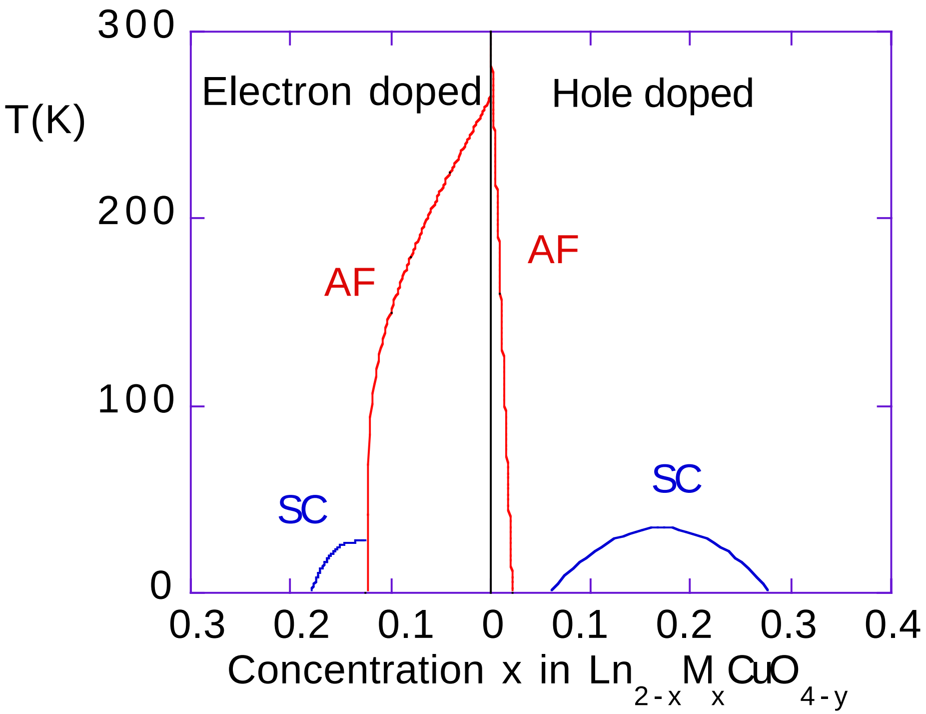

A Theoretical suggestion

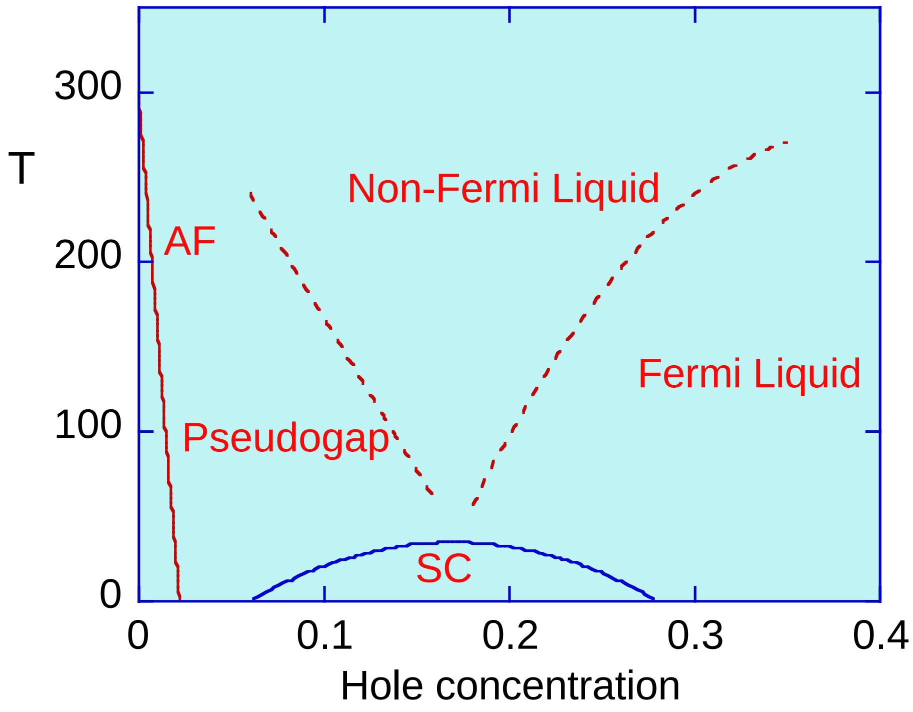

電気抵抗の温度依存性

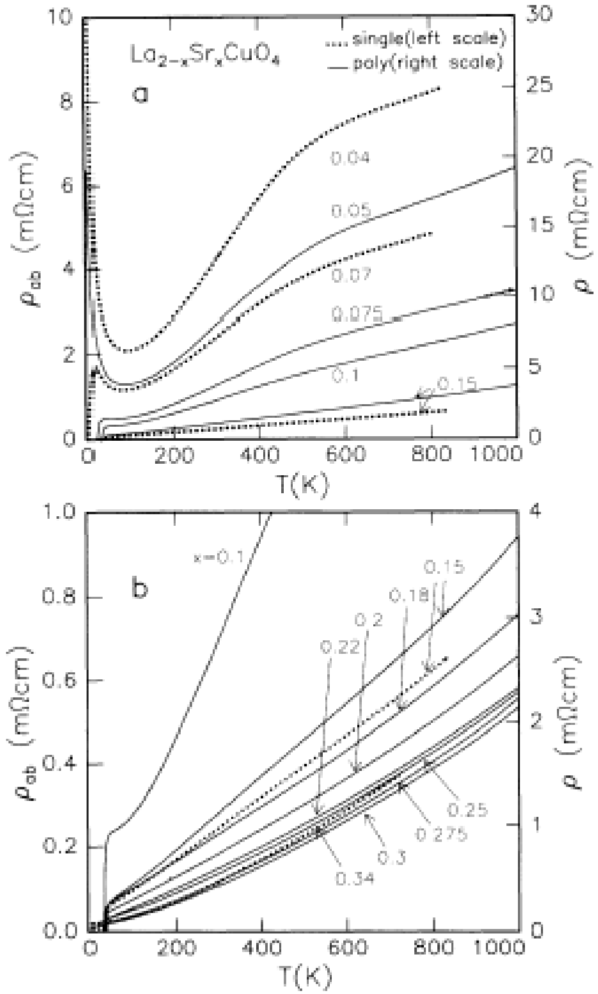

FIG. 1. The temperature dependence of the resistivity for $La_{2-x}Sr_xCuO_4$. (a) $0 < x \le 0.15$, (b) $0.1 \le x < 0.35$. Dotted lines, the in-plane resistivity (ρ_{ab}) of single-crystal films with (001) orientation; solid lines, the resistivity (ρ) of polycrystalline materials. Note, $\rho_M = (h/e^2)d = 1.7$ mΩ cm.

H. Takagi et al. PRL (1992)

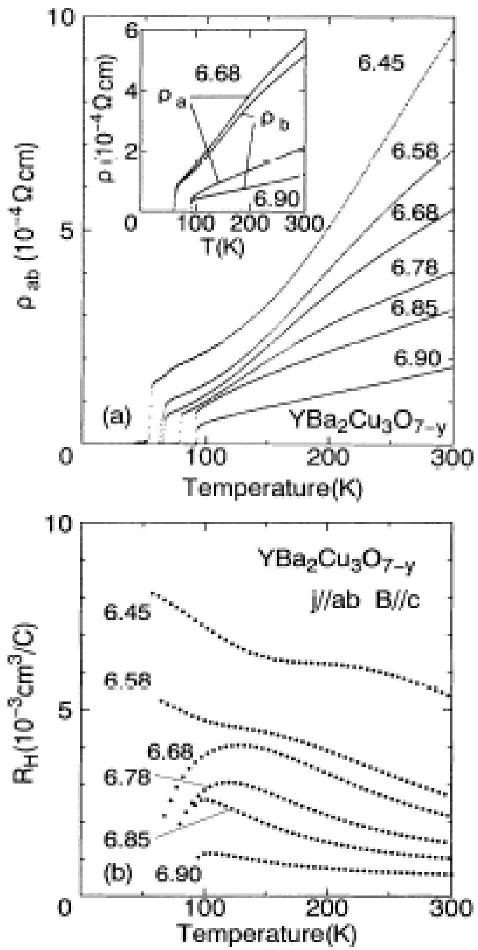

FIG. 1. (a) Temperature dependence of in-plane resistivity of twinned $YBa_2Cu_3O_{7-y}$ crystals with oxygen concentration $7-y \sim 6.90$, 6.85, 6.78, 6.68, 6.58, and 6.45. Inset: Temperature dependence of ρ_a and ρ_b for detwinned crystals of T_c=90 and 60 K. (b) Temperature dependence of R_H of twinned crystals measured under $\mathbf{j} \parallel ab$ plane and $\mathbf{B} \parallel c$ axis at $B = 5$ T.

T. Ito et al. PRL(1991)

比熱

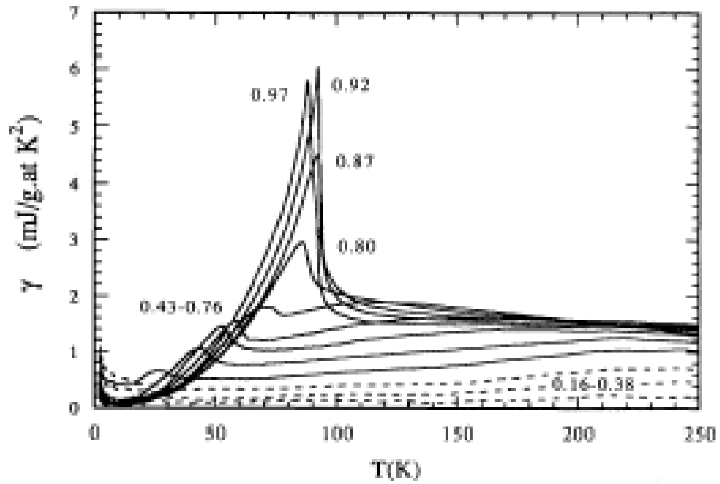

FIG. 4. Electronic specific heat coefficient $\gamma(x,T)$ vs T for $YBa_2Cu_3O_{6+x}$ relative to $YBa_2Cu_3O_6$. Values of x are 0.16, 0.29, 0.38, 0.43, 0.48, 0.57, 0.67, 0.76, 0.80, 0.87, 0.92, and 0.97.

Loram et al., Phys. Rev. Lett. 71, 1740 (1993)

LSCO

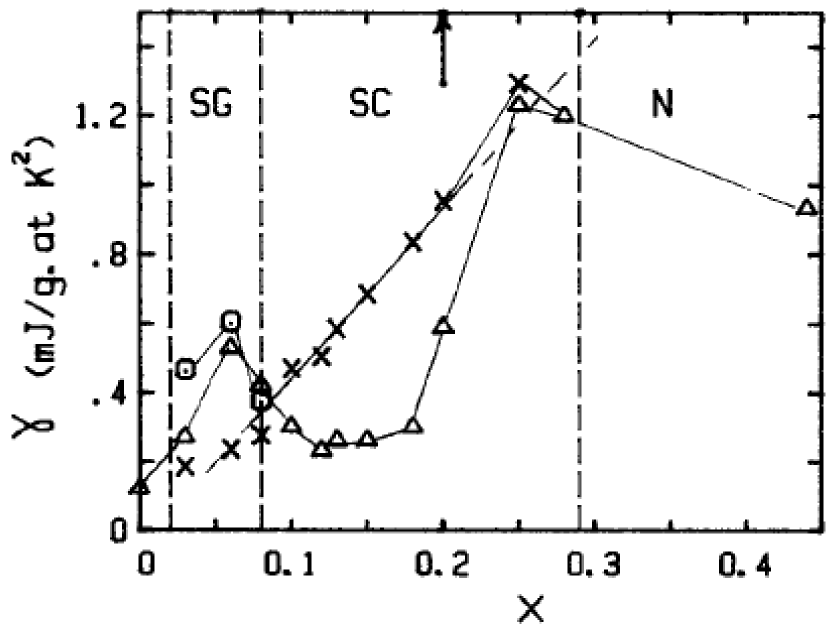

FIGURE 2

γ vs x. for x≤.08 Δ,γ (2K); o,γ (8K); x,γ (40K)
for x≥.1 Δ,γ(0); x, γ_n

Loram et al., Physica C162-164, 498 (1989)

磁気緩和率

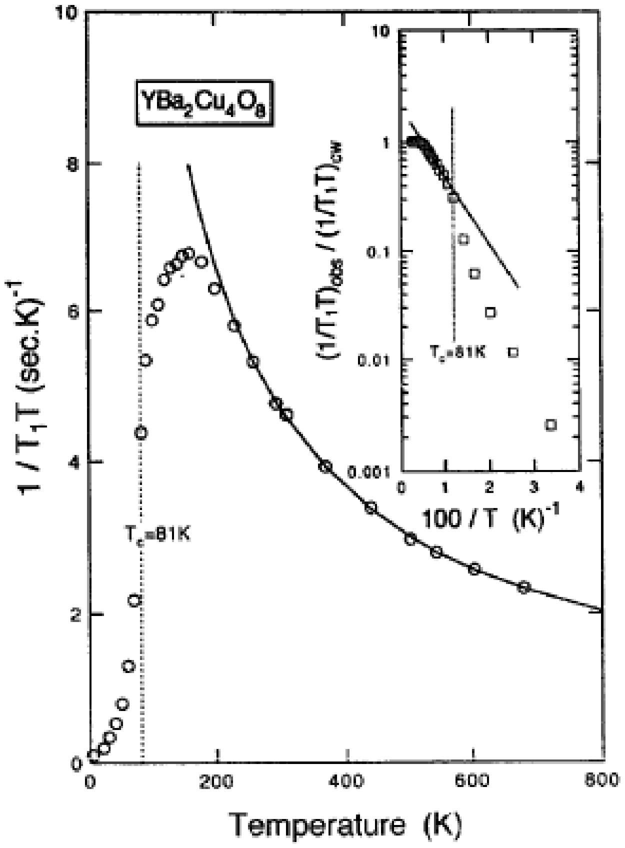

Fig. 1. Temperature dependence of the nuclear spin-lattice relaxation rate $1/T_1T$ for Cu(2) sites of $YBa_2Cu_4O_8$. The solid curve shows the best fit of the data to Eq. (1) for $T > 250$ K. The inset shows the Arrhenius plots for the ratio of the observed $(1/T_1T)_{obs}$ to the expected $(1/T_1T)_{cw}$ from Eq. (1), and the best fit of the data to Eq. (2) is shown by the solid line.

Yasuoka et al., Physica B199 (1994)278

$YBa_2Cu_4O_8$

アンダードープ域　T_c= 81K

Tcより上の温度から帯磁率が下がりはじめる。

擬ギャップ

スピンゆらぎ理論によると

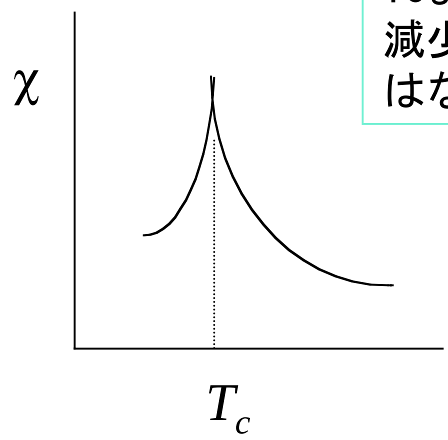

Tcより上から減少することはない。

量子臨界現象

量子相転移

- $T = 0$で起こる相転移
- 量子ゆらぎが重要

  量子ゆらぎにより引きおこされる
- 圧力、磁場変化、元素置換等による相転移
- 量子臨界点（相転移点）の近くでは非フェルミ流体の振る舞いが見られることがある。

  抵抗、比熱、帯磁率

スピンゆらぎ理論（Millis, Moriya）

3D	C/T	$\chi(Q)$	ρ	$1/T^{1}T$
Ferro.	$-\ln T$	$T^{-4/3}$	$T^{5/3}$	$T^{-4/3}$
AF	$T^{1/2}$	$T^{-3/2}$	$T^{3/2}$	$T^{-3/4}$

2D	C/T	$\chi(Q)$	ρ	$1/T^{1}T$
Ferro.	$T^{-1/3}$	$(T\ln T)^{-1}$	$T^{4/3}$	$\chi(Q)^{3/2}$
AF	$-\ln T$	T^{-1}	T	T^{-1}

（『重い電子系の物理』（大貫·上田より））

•2D Ferroについては、χ^{-1}は$T^{-4/5}$であり、低温でCurie-Weissとする文献もある。$1/T^{1}T \sim \chi^{3/2}$は一致している。

3. Hubbard Model
- Metal-Insulator Transition -

Itinerant Electrons

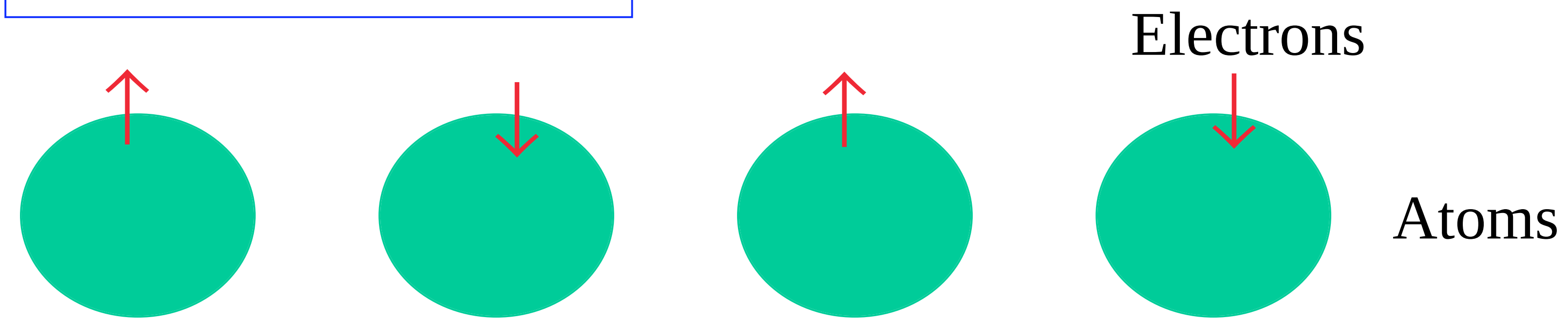

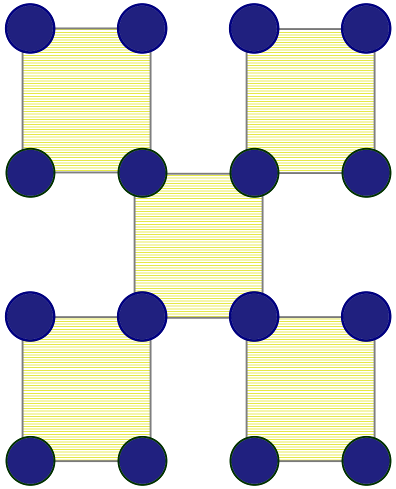

Square Lattice

Mott transition

MnO, FeO, CoO, Mn_3O_4, Fe_3O_4, NiO, CuO

Insulator: Coulomb interaction is Important !

Hubbard Model I

Coulomb interaction

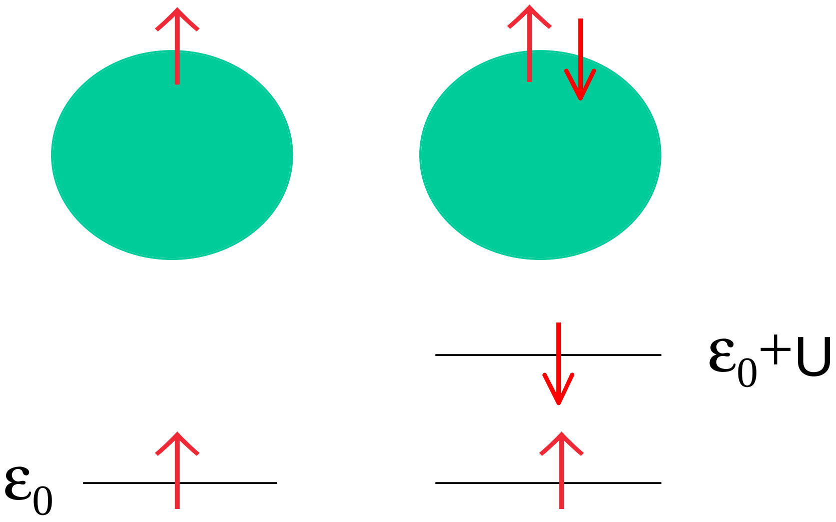

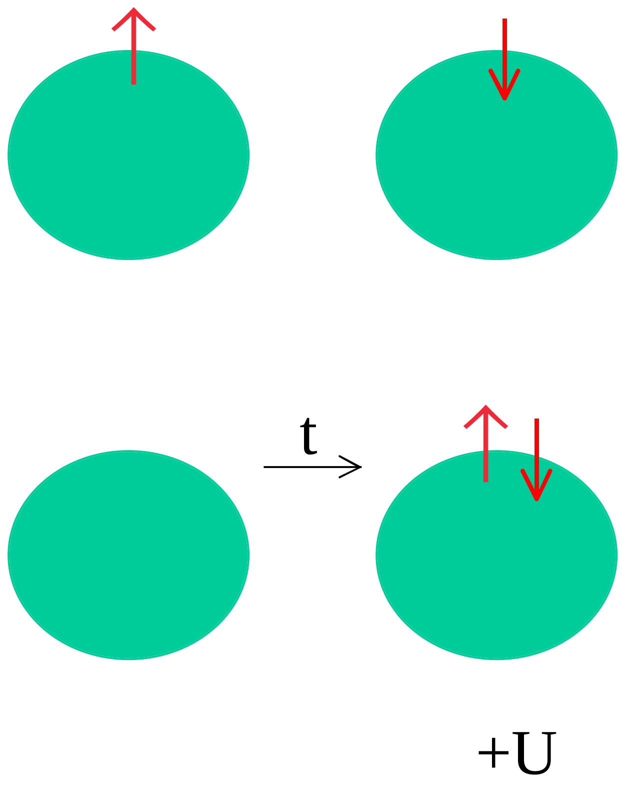

U >> t → Insulator

Hubbard Model II

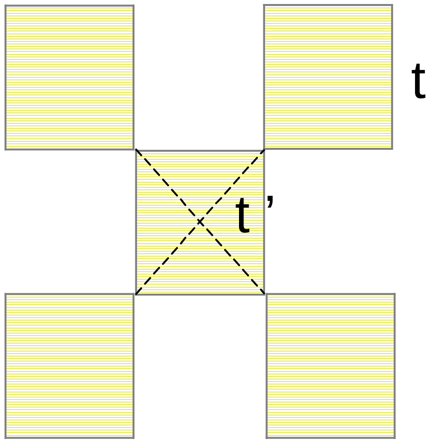

t'= 0

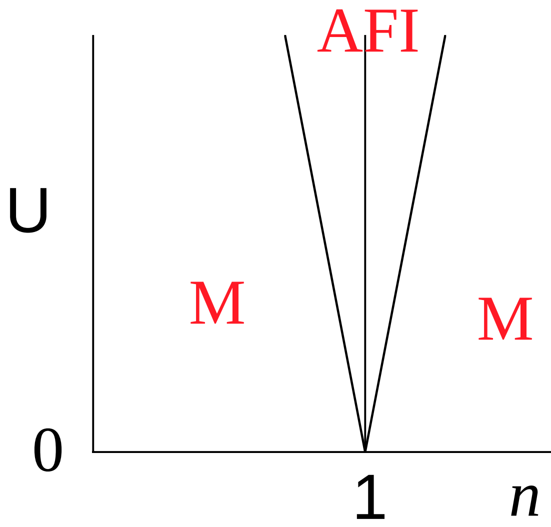

t'>0

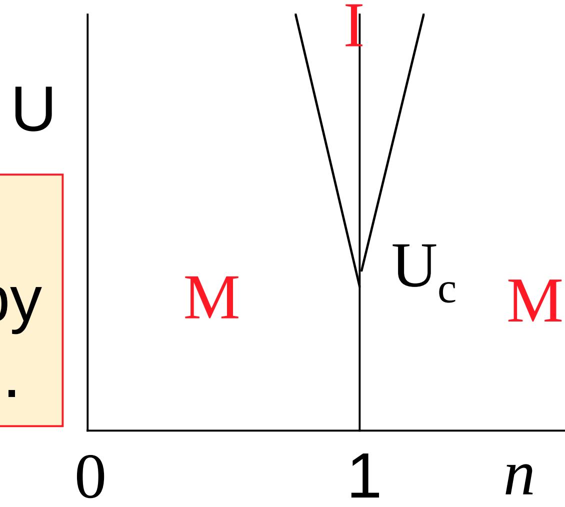

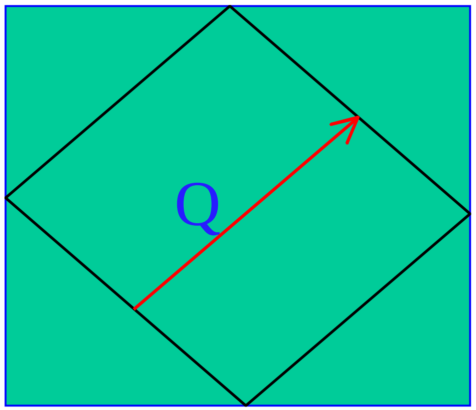

t' = 0

M-I transition
Is controlled by
n.n. transfer t'.

Hubbard Model III

Hartree-Fock theory (Half-filled)

AF Gap Δ = Um $\quad$ $D \sim t\, e^{-2\pi t/U}$ $\quad$ d = 1, 3

$\sim t\, e^{-2\pi (t/U)^{1/2}}$ $\quad$ d = 2

1D Hubbard model

		U << t	U >> t
Hubbard gap	Δ	$(16/\pi)\sqrt{tU}e^{-\pi/(2U)}$	U
Spin-wave velocity	$2v_s/\pi = J$	$(4t/\pi)(1-U/4\pi t)$	$4t^2/U$

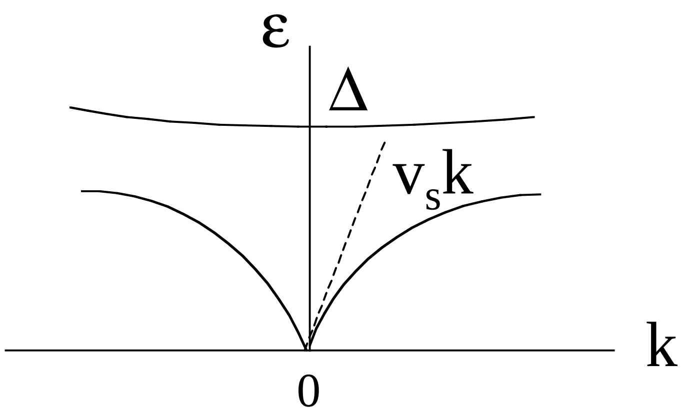

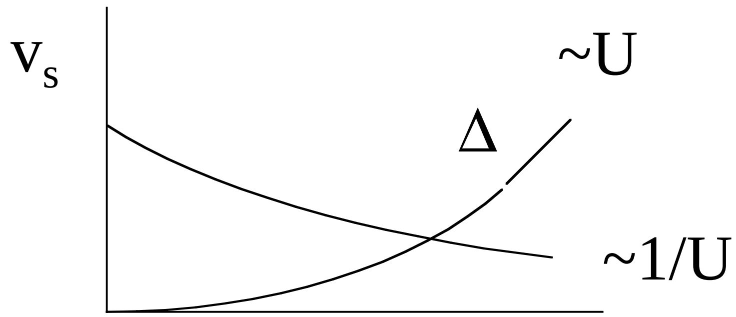

Mapping of the Hubbard Model

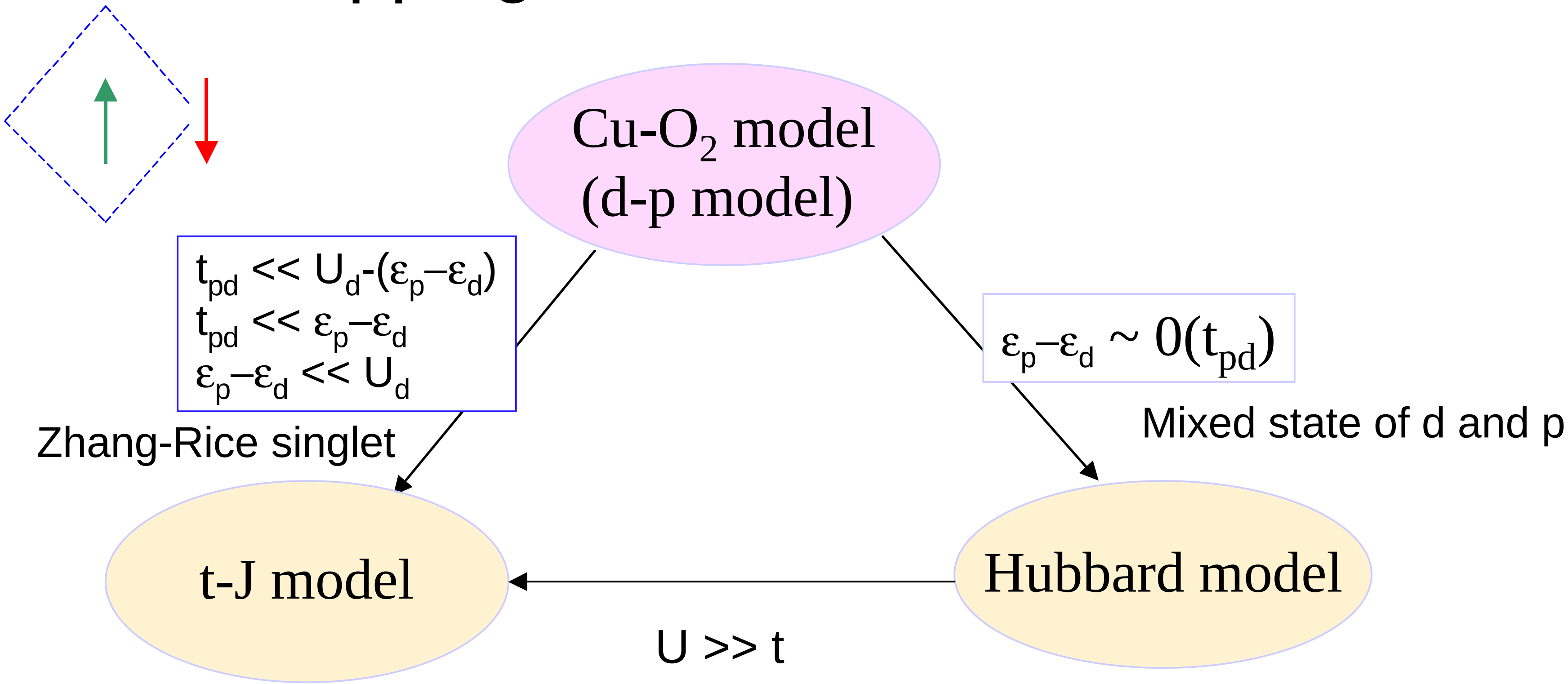

$$H = -t \sum_{\langle ij \rangle \sigma} (c_{i\sigma}^{+} c_{j\sigma} + h.c.) + J \sum_{\langle ij \rangle} S_i \cdot S_j$$

- Non-dopingでは絶縁体
- 反強磁性絶縁体にドープされたホールのモデル

$$H = -t \sum_{\langle ij \rangle \sigma} (c_{i\sigma}^{+} c_{j\sigma} + h.c.) + U \sum_{i} n_{i\uparrow} n_{i\downarrow}$$

- 金属ー絶縁体転移のモデル
- pホールはdと強く混成するモデル

d-p Model

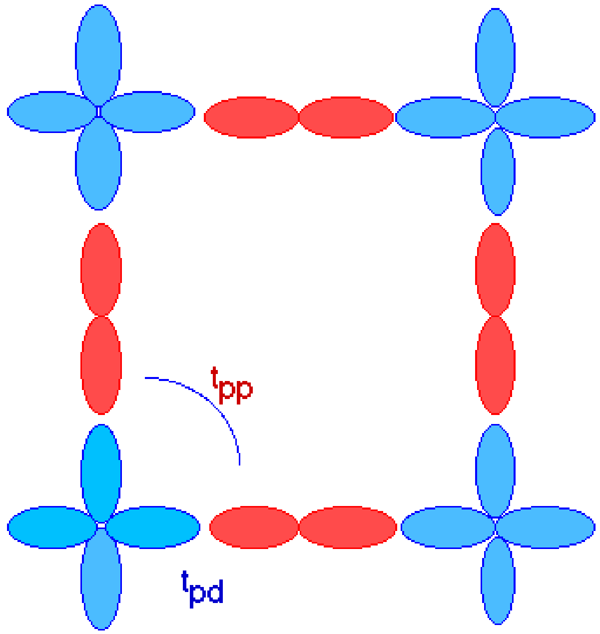

Model for CuO_2 plane

Non-doping (half-filling) case

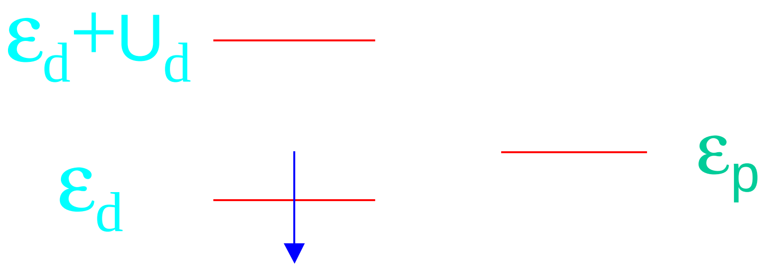

Antiferromagnetic Insulator

Charge transfer insulator

(Mott insulator) *if*

$$\varepsilon_p - \varepsilon_d >> t_{pd}$$

Superconductivity in the Hubbard model

Question

Superconductivity in the Hubbard model is possible ?

- YES
  - Perturbation
  - FLEX
  - VMC some QMC
- NO
  - QMC, CPMC

4. Variational Monte Carlo method

適当な波動関数の期待値をモンテカルロ法により計算する

Gutzwillerただ $\psi_G = P_G \psi_0$

ψ_0 ：試行関数　フェルミ球、反強磁性、超伝導

$$P_G = \prod_j \left(1-(1-g)n_{j\uparrow}n_{j\downarrow}\right)$$ Gutzwiller演算子

$$0 \le g \le 1$$

パラメータgによりオンサイトの相関を制御する

weight g
Coulomb +U

weight 1

VMC –計算方法–

Normal state ψ_0 Slater 行列式

$$\psi_0 = \sum_{l} a_l \psi_l$$

ψ_l ： 実空間での粒子の配置

波数 $k_1, k_2, \ldots, k_n$ 座標 $j_1, j_2, \ldots, j_n$ を↑粒子が占めている時

$$\det D_\uparrow = \begin{vmatrix} e^{ik_1 j_1} e^{ik_1 j_2} \cdots e^{ik_1 j_n} \\ \cdots \\ e^{ik_n j_1} e^{ik_h j_2} \cdots e^{ik_n j_n} \end{vmatrix}$$

Slater 行列式

ウェイト $a_l = \det D_\uparrow \det D_\downarrow$

粒子の配置の総数は大きな数 → モンテカルロ法

モンテカルロ法

期待値

$$\langle \psi Q \psi \rangle = \sum_{mn} a_m a_n \langle \psi_m Q \psi_n \rangle = \sum_m \frac{a_m^2}{\sum_l a_l^2} \sum_n \frac{a_n}{a_m} \langle \psi_m Q \psi_n \rangle$$

ψ_m の出現確率が $P_m = \frac{a_m^2}{\sum_l a_l^2}$ に比例するようにサンプルを生成すると

$$\langle \psi Q \psi \rangle = \frac{1}{M} \sum_m \left(\sum_n \frac{a_n}{a_m} \langle \psi_m Q \psi_n \rangle \right) \qquad m = 1, \ldots, M$$

Metropolis法 ψ_j の次に ψ_n を生成した時（例えば、どれかの電子を動かす）

$R = |a_n|^2 / |a_j|^2 \geq \xi$ なら ψ_n を採用

$< \xi$ ψ_j のまま

ξ: 一様乱数 $0 \leq \xi < 1$

$\langle \psi_m Q \psi_n \rangle$ の計算には余因子展開を使うとcpu時間を稼げる

超伝導状態のVMC

$$\Psi_s = P_N P_G \psi_{BCS}$$

$$\psi_{BCS} = \prod_k (u_k + v_k c^+_{k\uparrow} c^+_{-k\downarrow})|0\rangle$$

P_N： 電子数をN個に固定

$$\Psi_s = P_G P_N \exp\left(\sum_k \frac{v_k}{u_k} c^+_{k\uparrow} c^+_{-k\downarrow}\right)|0\rangle$$

$$= P_G \left(\sum_k \frac{v_k}{u_k} c^+_{k\uparrow} c^+_{-k\downarrow}\right)^{N/2} |0\rangle$$

$$= P_G \left(\sum_k a_{ij} c^+_{i\uparrow} c^+_{j\downarrow}\right)^{N/2} |0\rangle$$

$$a_{ij} = \frac{1}{V} \sum_k \frac{v_k}{u_k} e^{ik\cdot(R_i - R_j)}$$

$N_\uparrow = N_\downarrow$ の時

↑電子が$i_1, i_2, .. i_{N/2}$; ↓電子が$j_1, j_2, .. j_{N/2}$
にいる時、ウェイトは行列式

$$\begin{vmatrix} a_{i_1 j_1} & \mathrm{L} & a_{i_1 j_{N/2}} \\ \mathrm{L} & & \\ a_{i_{N/2}} & \mathrm{L} & a_{i_{N/2} j_{N/2}} \end{vmatrix}$$

で与えられ、normal stateと同様に計算できる。

♠ 一般のペアー状態は、近藤さんのレクチャーにあるように、一つのSlater行列式では書けないが、BCS状態は一体近似をしているので、行列式で書くことができる。

ニュートン法

エネルギーE($x_1,\ldots,x_n$)の極小　パラメータ$x=(x_1,\ldots,x_n)$

微分　$f_j(x)=\dfrac{\partial E}{\partial x_j}(x)$　がゼロとなる点を探す

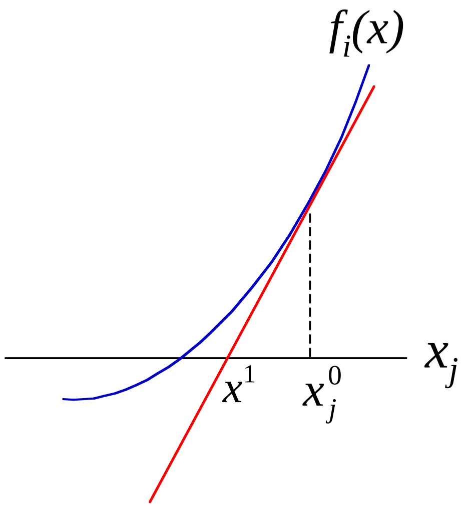

初期値 x_0に対しニュートン法により

$$f_i(x^0)+\sum_j \frac{\partial f_i}{\partial x_j}(x^0)(x_j-x_j^0)=0$$

を満たすx^1が次の候補。

$$H_{ij}=\frac{\partial f_i}{\partial x_j}(x^0)=\frac{\partial^2 E}{\partial x_j \partial x_i}(x^0)$$

とおくと

$$\begin{pmatrix} x_1^1 \\ x_2^1 \\ . \\ . \end{pmatrix}=\begin{pmatrix} x_1^0 \\ x_2^0 \\ . \\ . \end{pmatrix}-H^{-1}\begin{pmatrix} f_1(x^0) \\ f_2(x^0) \\ . \\ . \end{pmatrix}$$

H_{ij} ：ヘッセ行列　数値的に計算する

Superconducting state

SC state in the correlated electron system: finite U

$$\psi_{CdS} = P_G \prod_k (u_k + v_k c^+_{k\uparrow} c^+_{-k\downarrow}) |0\rangle$$

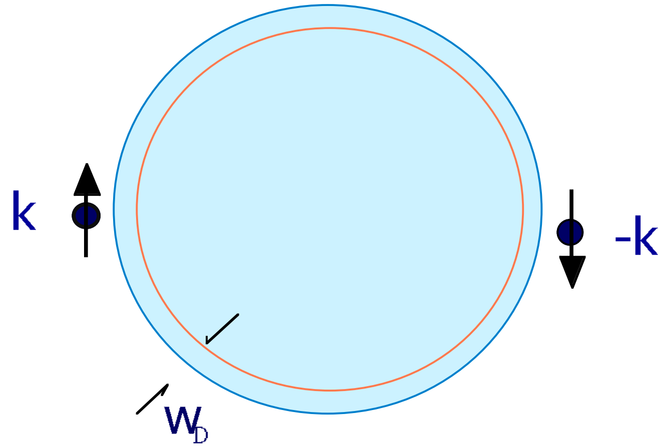

Gutzwiller Projection P_G

To control the on-site strong correlation

Weight g
Coulomb +U

Weight 1
Parameter 0<g<1

Essentially Equivalent
to
RVB state (Anderson)

Relation to Gossamer superconductivity

Bogoliubov op. $b_{k\sigma}\psi_{BCS} = 0$

Projected op. $\tilde{b}_{k\sigma} = P_G b_{k\sigma} P_G^{-1}$

$$\tilde{H} = \sum_{k\sigma} E_k \tilde{b}^{+}_{k\sigma}\tilde{b}_{k\sigma} \qquad \tilde{b}_{k\sigma}\tilde{\psi}_{SC} = 0$$

Gossamer SC state $\tilde{\psi}_{SC}$

Laughlin cond-mat/0209269

In fact

$$\tilde{\psi}_{SC} = P_G \psi_{BCS} \qquad \tilde{b}_{k\sigma} P_G \psi_{SC} = P_G b_{k\sigma}\psi_{BSC} = 0$$

Gossamer superconductivity
= Projected BCS state

Superconducting condensation energy

SC Condensation energy

$$\Delta E_{SC} = \Omega_n - \Omega_s = \int_0^{T_c} (S_n - S_s) dT$$

$$= \int_0^{T_c} (C_s - C_n) dT$$

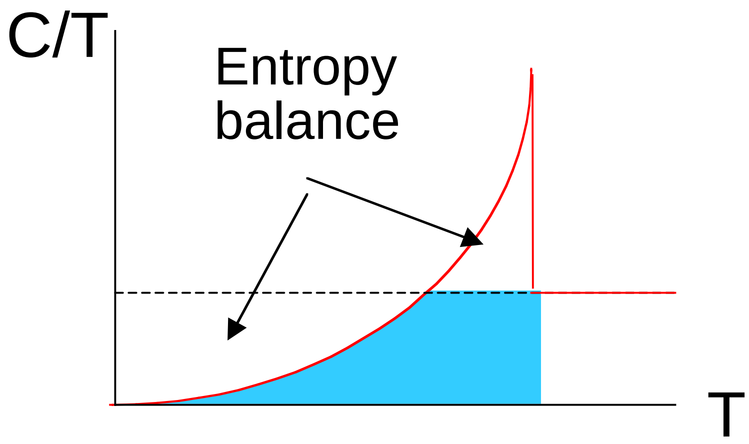

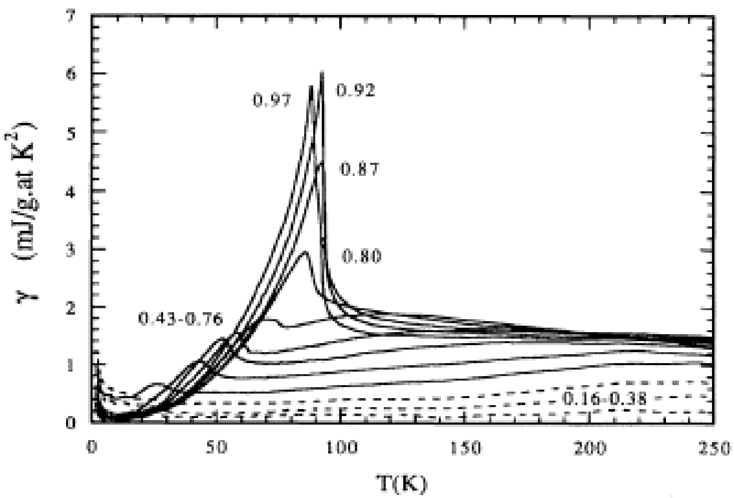

FIG. 4. Electronic specific heat coefficient $\gamma(x,T)$ vs T for $YBa_2Cu_3O_{6+x}$ relative to $YBa_2Cu_3O_6$. Values of x are 0.16, 0.29, 0.38, 0.43, 0.48, 0.57, 0.67, 0.76, 0.80, 0.87, 0.92, and 0.97.

Loram et al. PRL 71, 1740 (‘93)

optimally doped YBCO

SC Condensation energy
~ 0.2 meV

Evaluations in the superconducting state

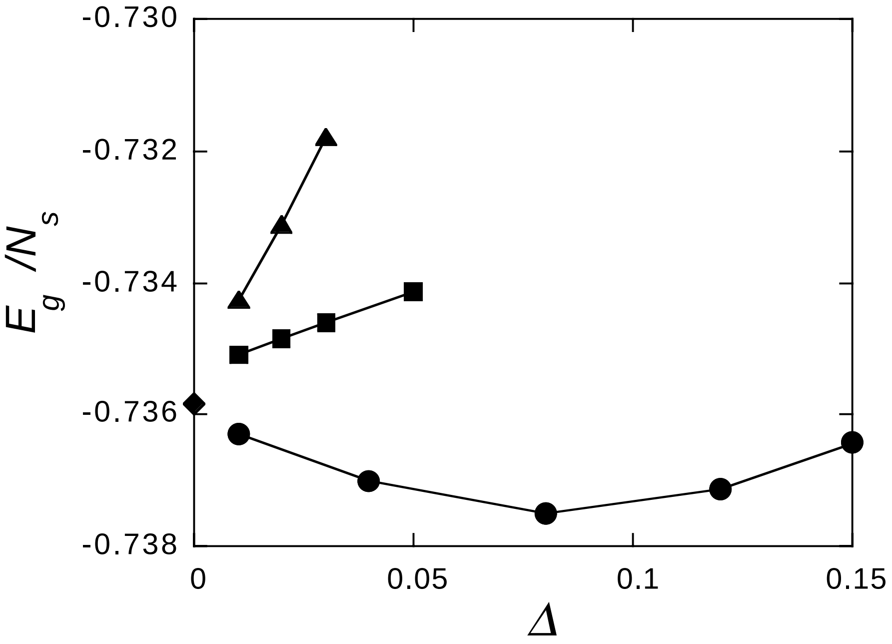

Variational Monte Carlo

10x10 U= 8

T. Nakanishi et al.
JPSJ 66, 294 (1997)

K. Yamaji et al.,
Physica C304, 225 (1998)
T. Yanagisawa et al.,
Phys. Rev. B67, 132408
(2003)

YBCO →

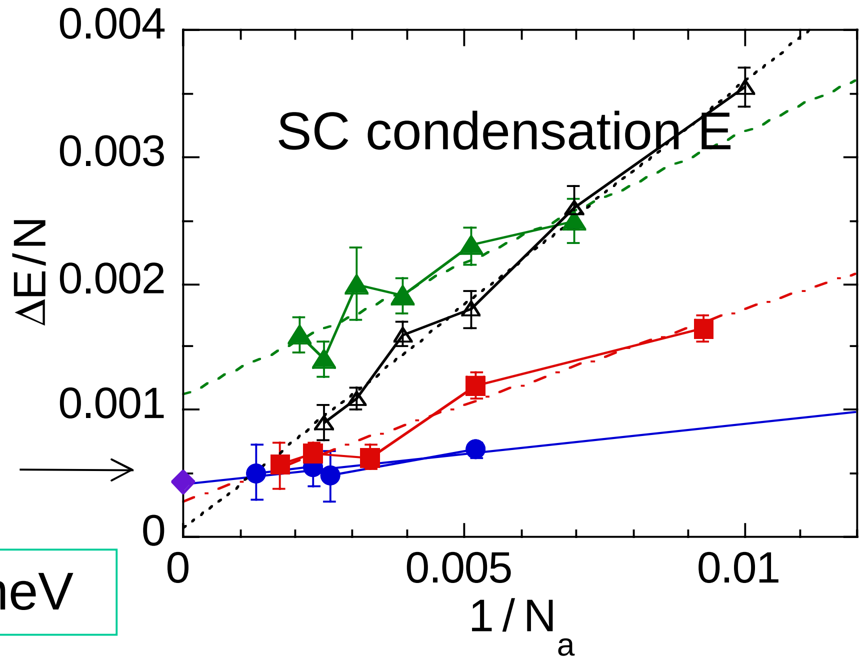

E_{cond} ~ 0.2meV

SC Condensation Energy for d-p model

Condensation energy

$E_{cond} \sim 0.00038 t_{dp}$
$= 0.56$ meV/site

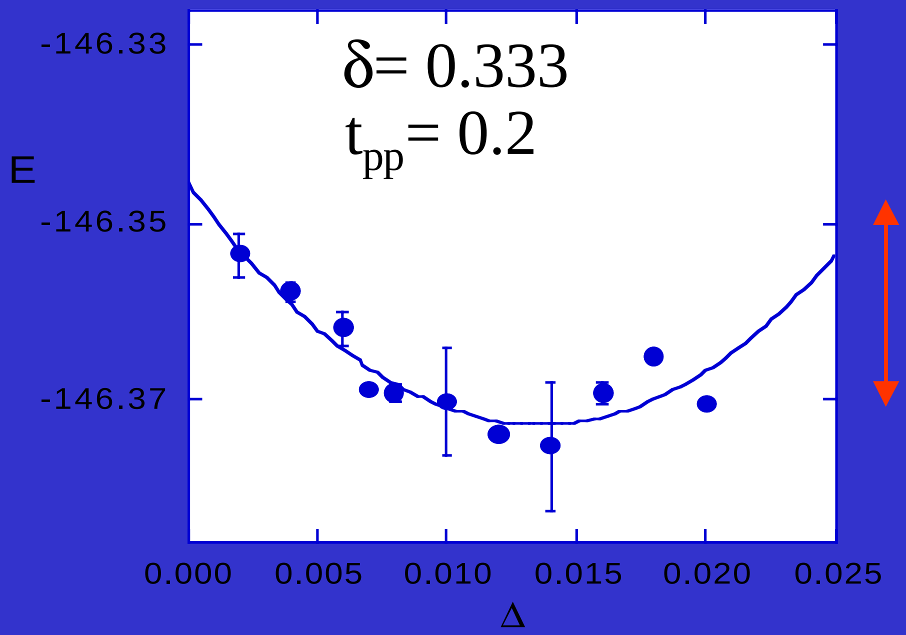

SC order parameter

2D 3-band model
6x6 and 8x8

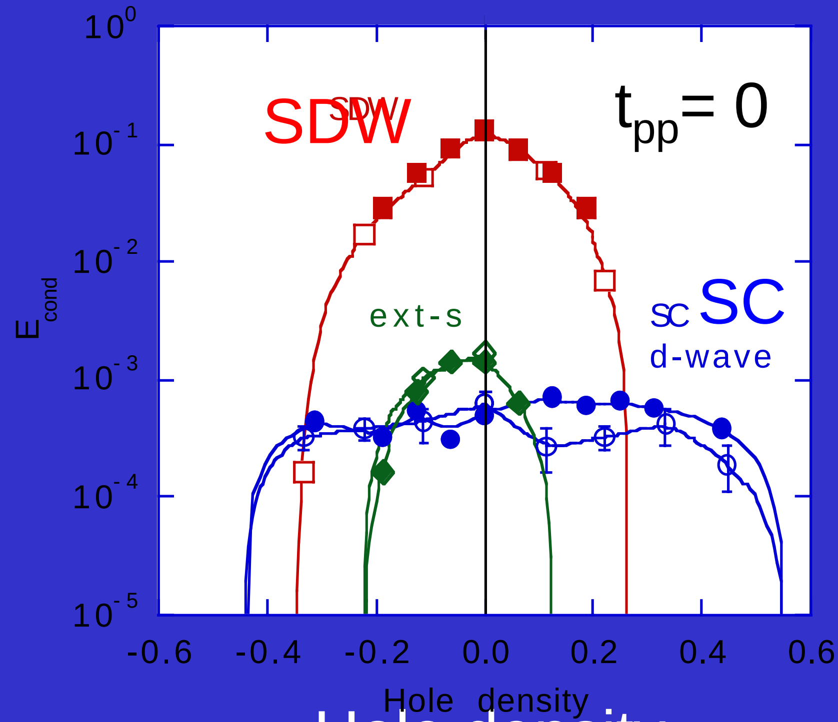

Hole density

T.Y. et al., PRB64, 184509 ('01)

5. Superconductivity and Antiferromagnetism

Competition

Size dependence of SC condensation energy

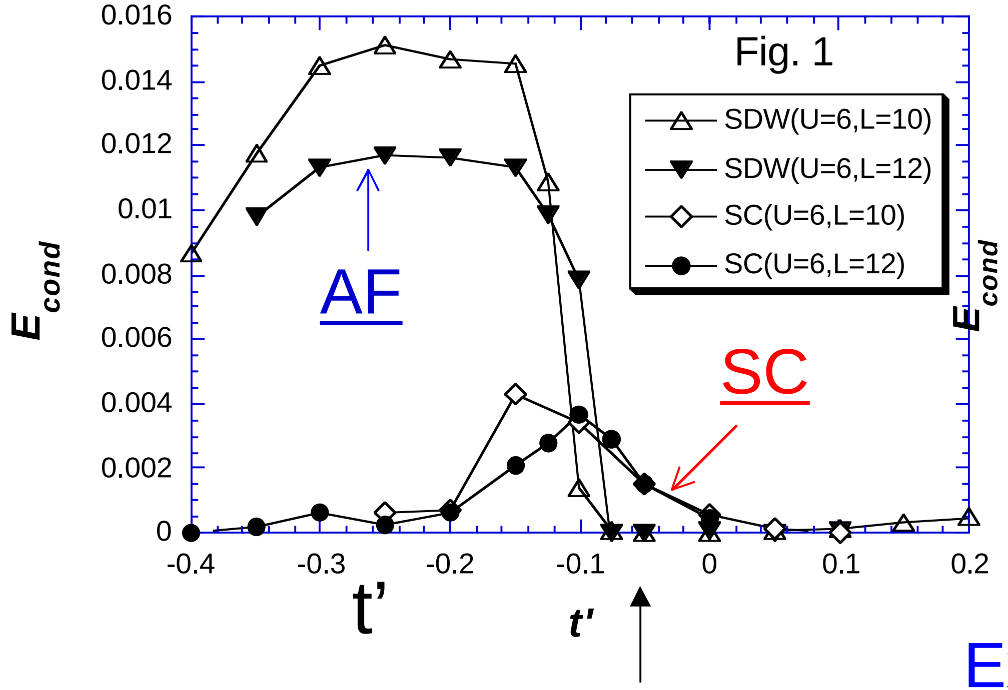

Pure d-wave SC

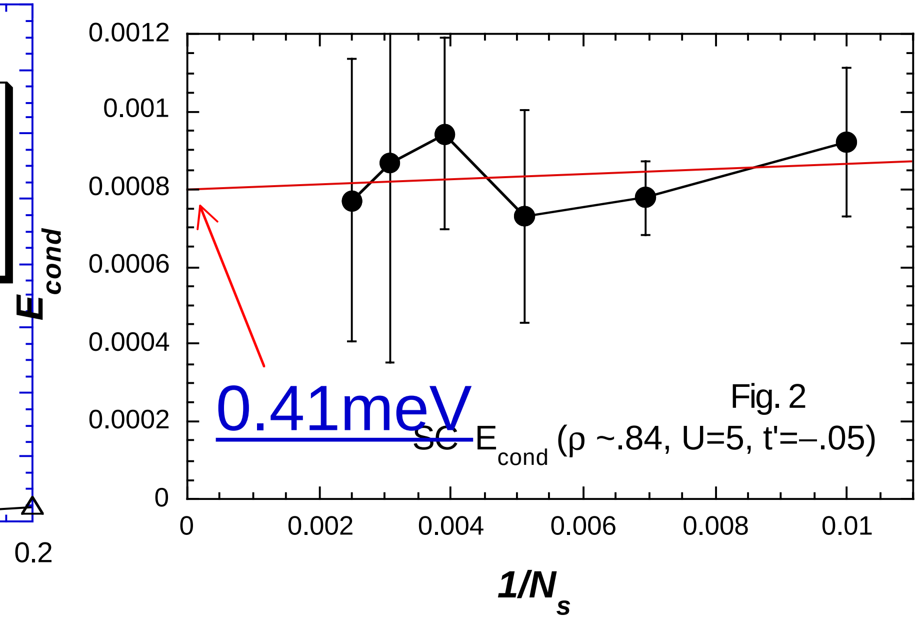

Experiments

0.26 meV/site (critical field H_c)

0.17~0.26 (C/T)

Bi2212とLSCO

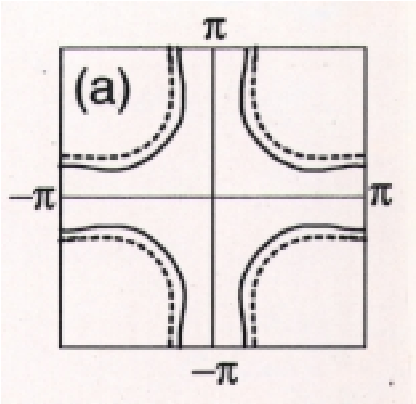

Bi2212型
t'/t = -0.34
t"/t = 0.23

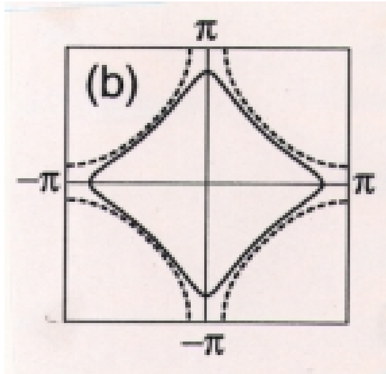

LSCO型
t'/t = -0.12
t"/t = 0.08

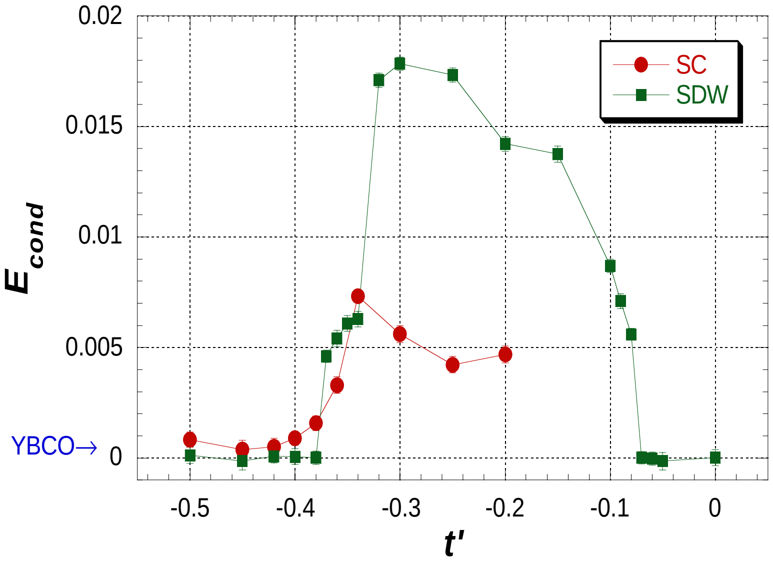

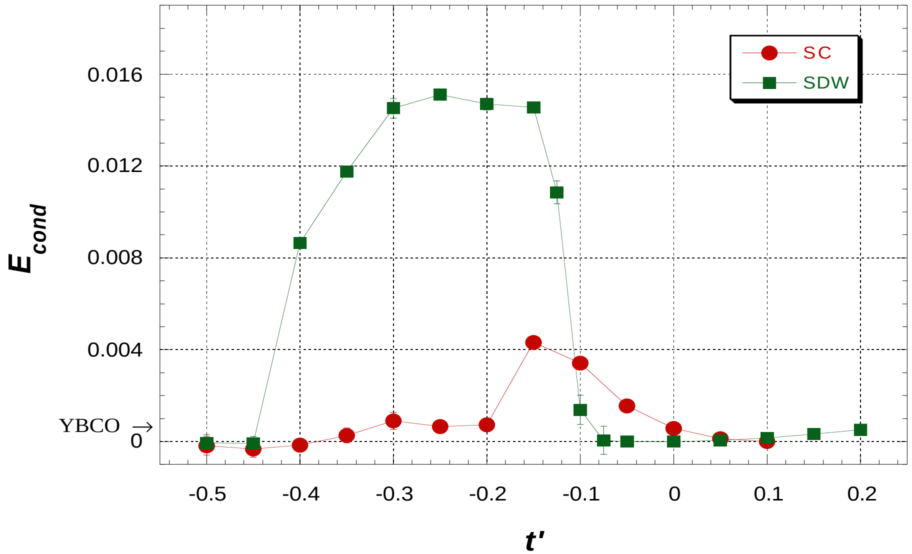

●と■: それぞれ絶対零度における超伝導と反強磁性凝縮エネルギー。
適切なパラメーター領域で超伝導●が反強磁性■に勝つ。

Gutzwiller-Jastrow function

Gutzwiller関数の改良

$$\psi_J = \prod_{\langle ij \rangle} \exp(-\alpha n_i n_j) P_G \psi_0$$

近接サイト間の相関

- エネルギーがかなり下がる
- 超伝導凝縮エネルギーが

増大する傾向あり

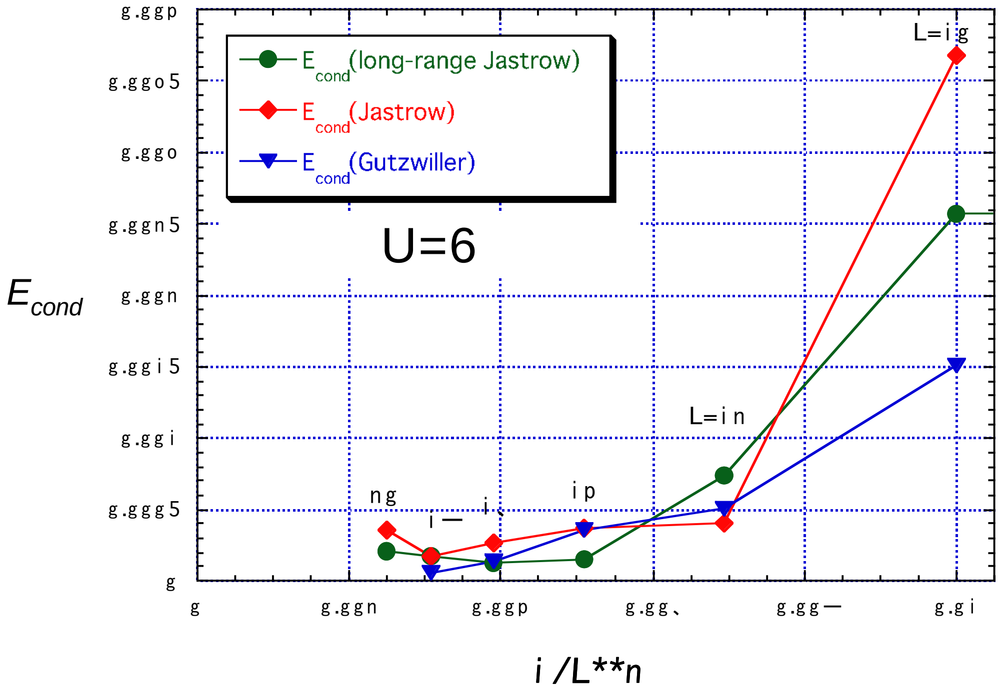

6. Stripes in high-Tc cuprates

- Vertical stripes for x > 0.05
- Diagonal stripes for x < 0.05

AF coexists with SC?

Neutron scattering

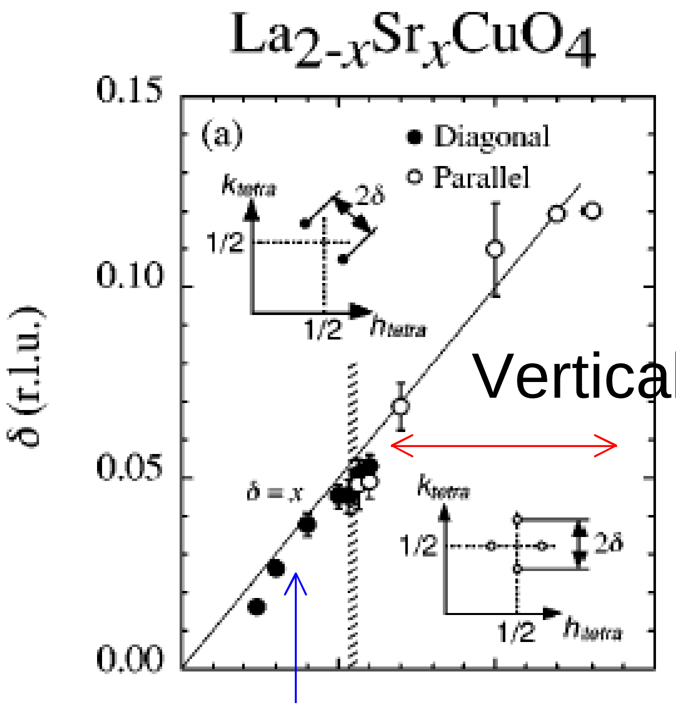

Vertical

Diagonal

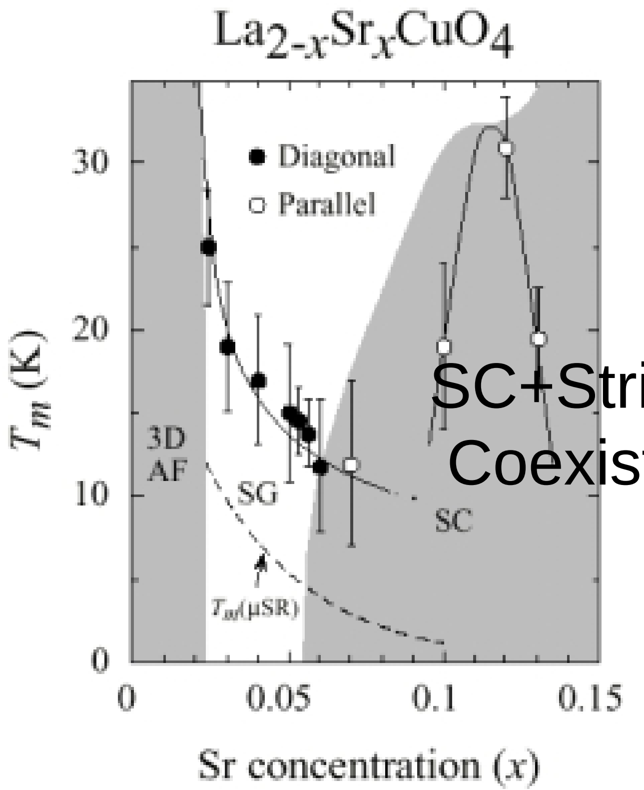

SC+Stripes Coexist

M.Fujita et al. Phys. Rev.B65,064505('02)

S.Wakimoto et al. PRB61, 3699('00)

Vertical Stripes in the under-doped region

Vertical stripes: 8 lattice periodicity (Tranquada)

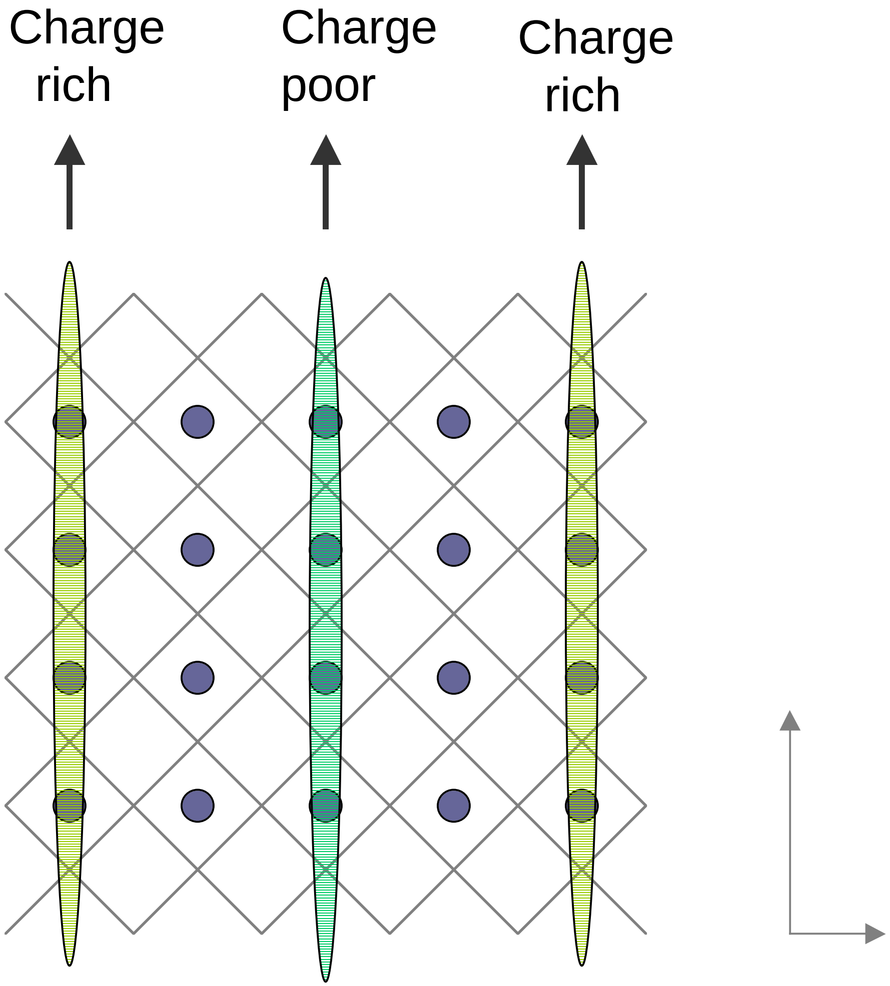

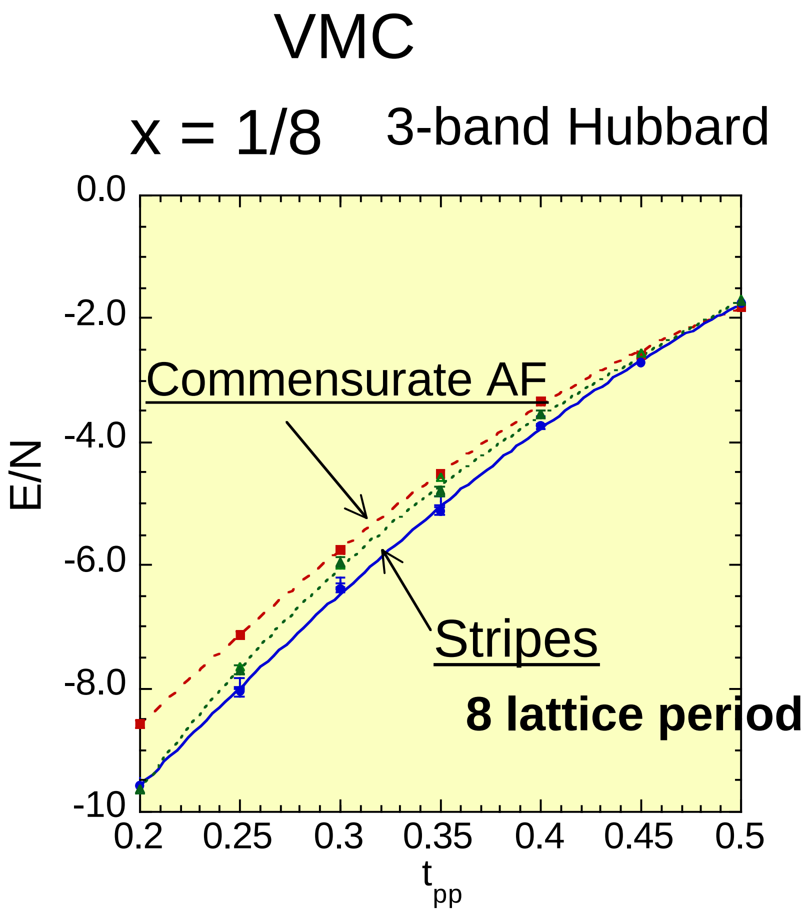

T.Y. et al., J.Phys.C14,21('02)

Stripes and Superconductivity: nano SC

Compete and Collaborate

SC coexists with stripes (AF).

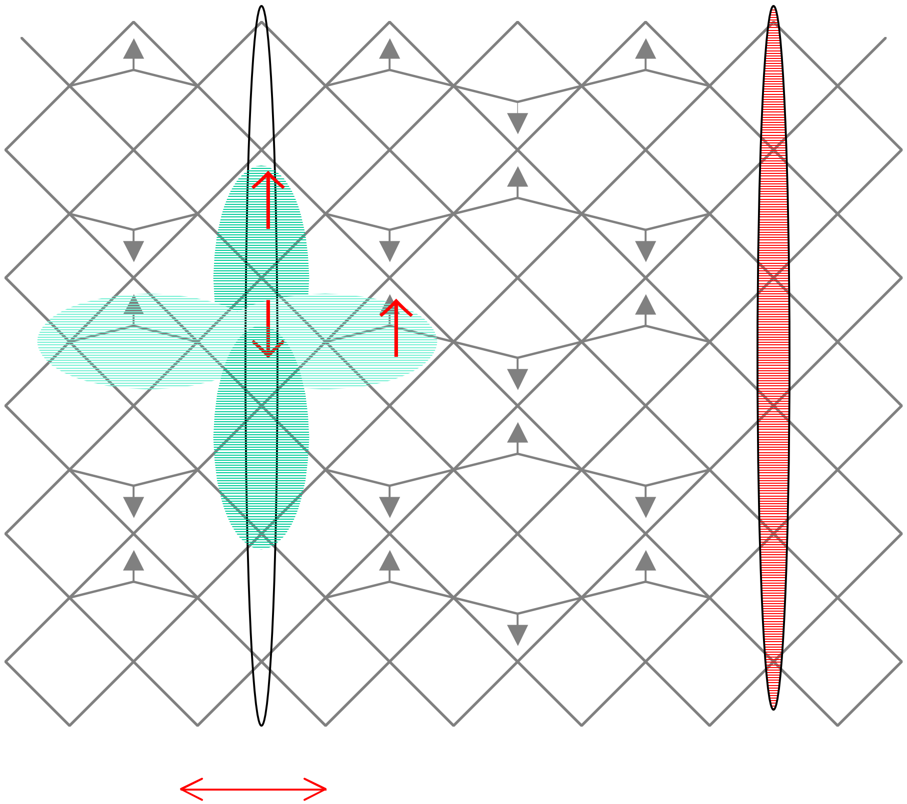

Nano-scale SC

Bogoliubov-de Gennes eq.

$$\begin{pmatrix} H_{ij\uparrow} + F_{ij} \\ F^*_{ji} - H_{ji\downarrow} \end{pmatrix} \begin{pmatrix} u_j^\lambda \\ v_j^\lambda \end{pmatrix} = E^\lambda \begin{pmatrix} u_i^\lambda \\ v_i^\lambda \end{pmatrix}$$

$$\alpha_\lambda = u_i^\lambda a_{i\uparrow} + v_i^\lambda a^+_{i\downarrow}$$

$$\overline{\alpha_\lambda} = \overline{u}_i^\lambda a_{i\uparrow} + \overline{v}_i^\lambda a^+_{i\downarrow}$$

Wave function

$$V_{\lambda j} = v_j^\lambda \qquad (\overline{U})_{\lambda j} = \overline{u}_j^\lambda$$

$$\psi_{SC} = P_G P_{N_e} \prod_\lambda \alpha_\lambda \overline{\alpha}^+_\lambda |0\rangle \propto P_G \left(\sum_{ij} (U^{-1}V)_{ij} a^+_{i\uparrow} a^+_{j\downarrow} \right)^{N_e/2} |0\rangle$$

SC coexists with Stripes

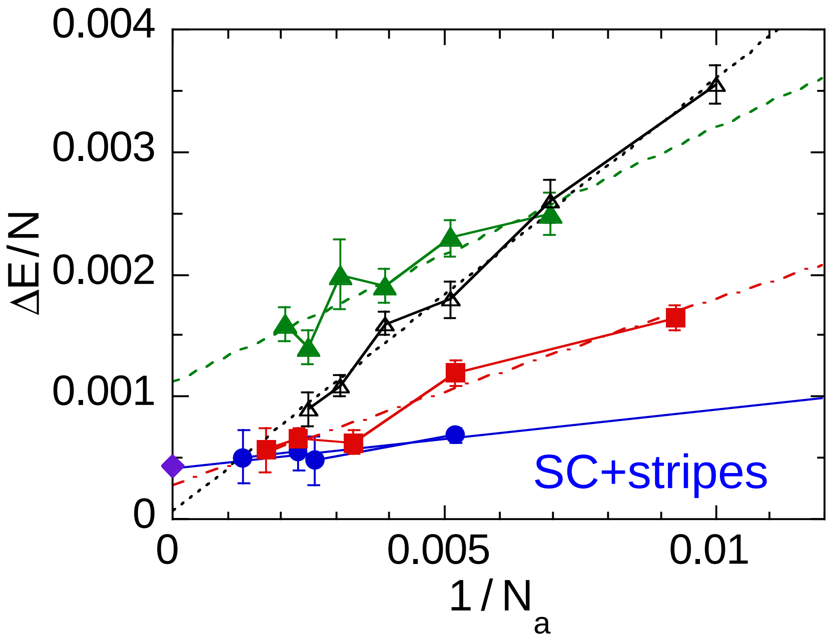

SC coexists with Antiferromagnetism and stripes.

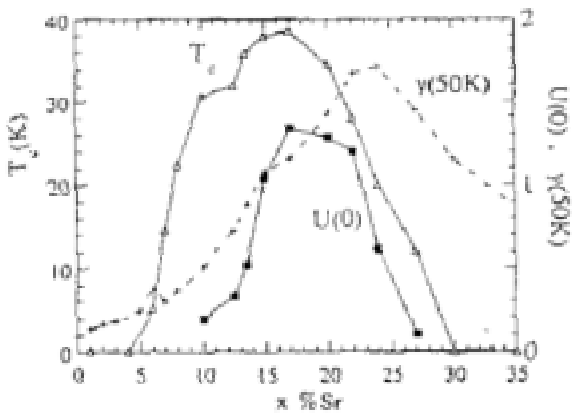

Figure 18 T_c, U(0) (J/g-at) and γ(50K) (mJ/g-at.K²) for $La_{2-x}Sr_xCuO_4$

Loram et al.

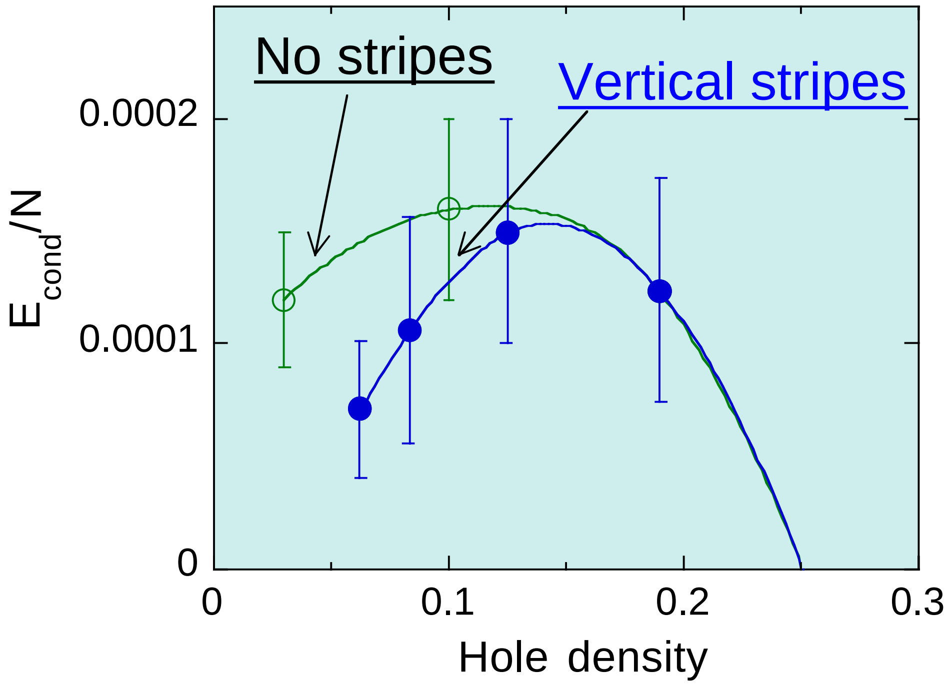

T. Y. et al., Phys. Rev. B67 (2003) 132408.

7. Diagonal stripes in lightly doped region

Diagonal stripes are observed for

$La_{2-x}Sr_xNiO_4$
$La_{2-x}Sr_xCuO_4$
$La_{2-x-y}Nd_ySr_xCuO_4$

in the lightly doped region.

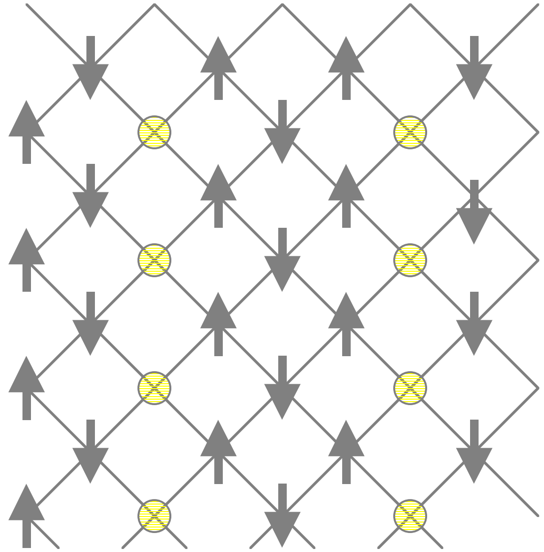

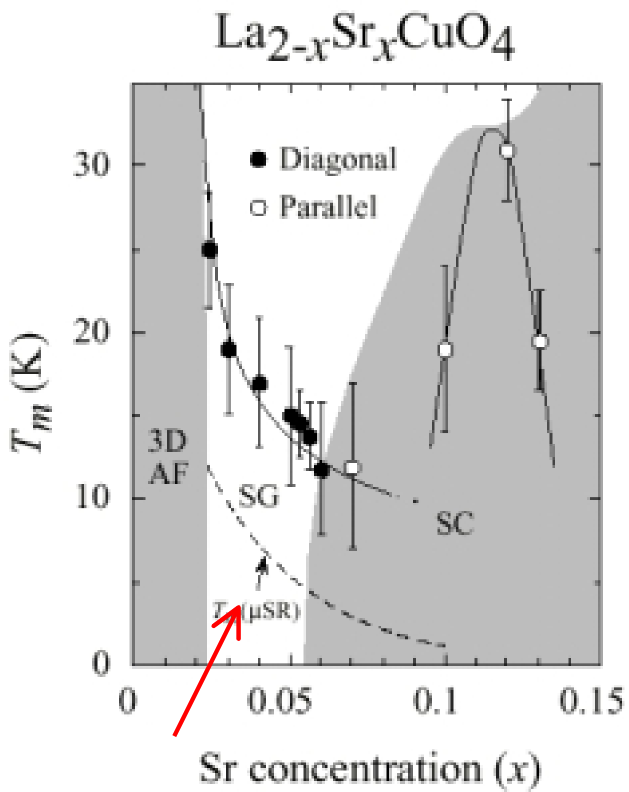

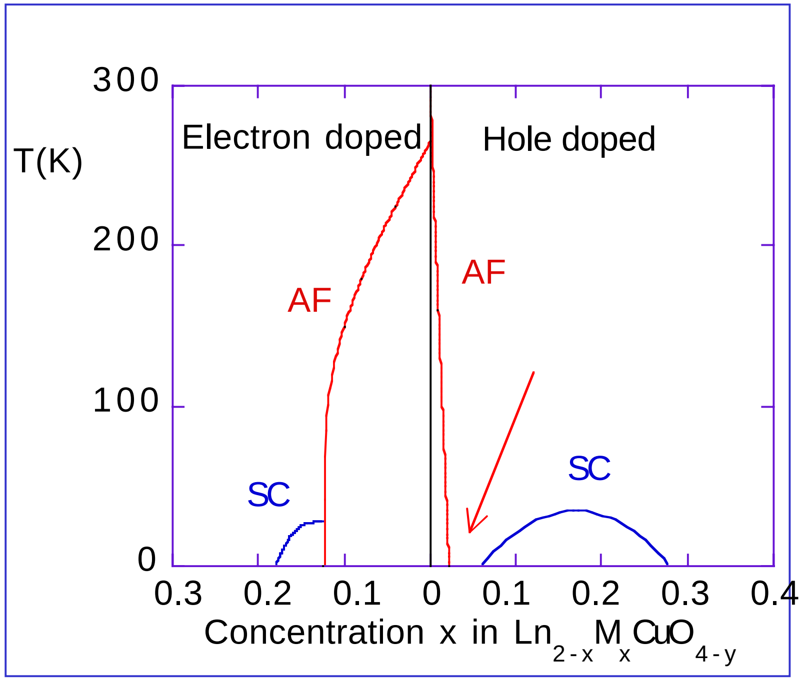

Types of stripes

Site-center Diagonal stripes (DS)

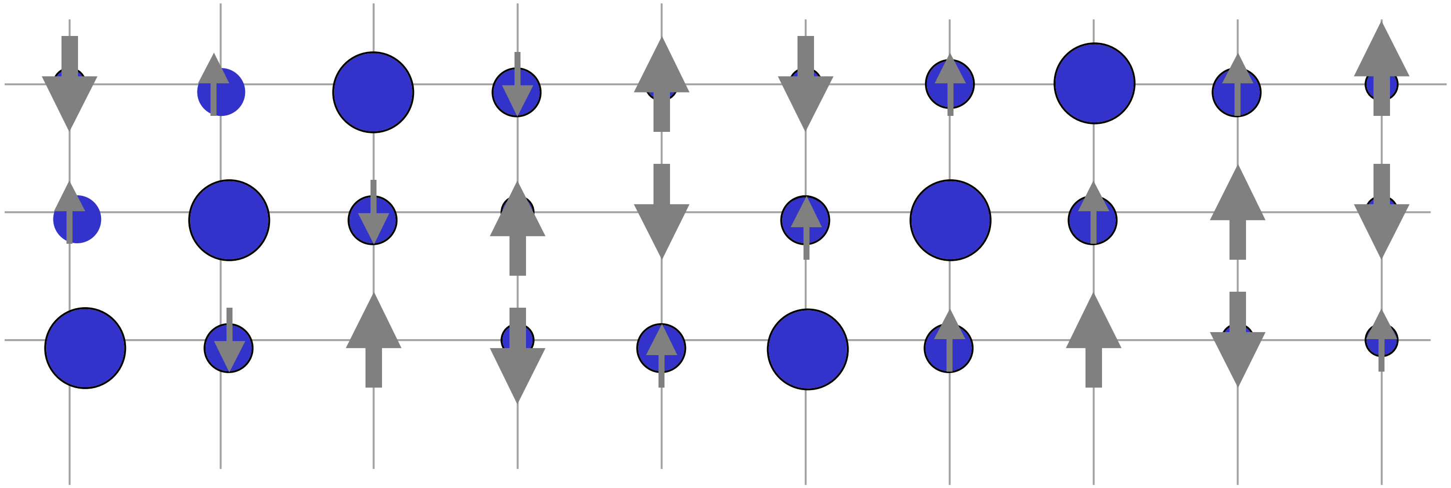

Bond-center Diagonal stripes (DB)

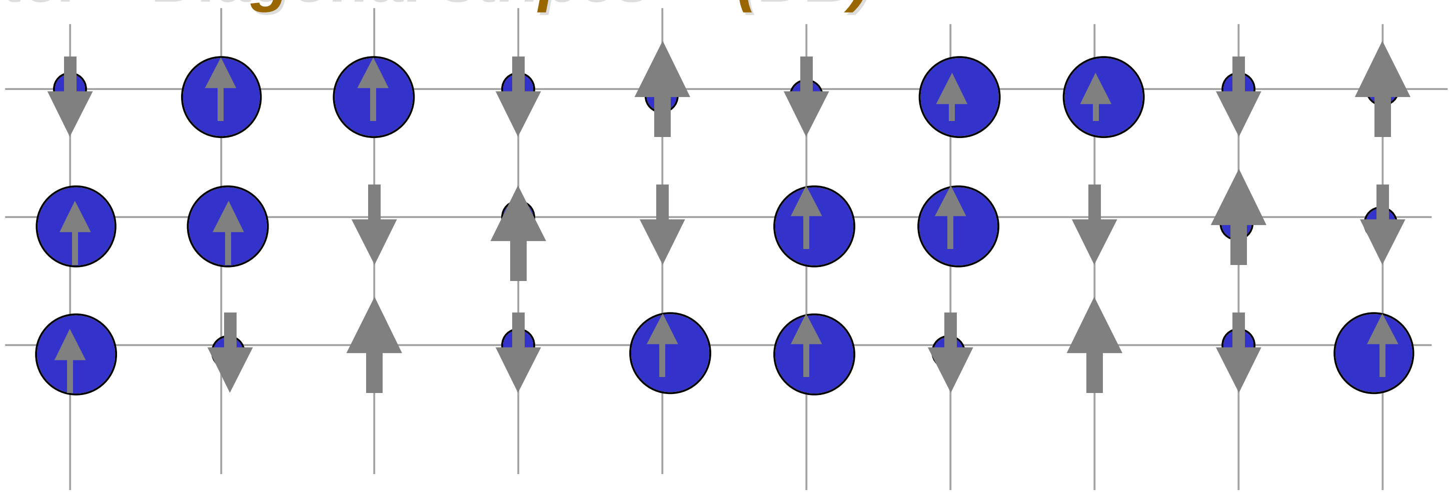

Total energy of diagonal striped state (VMC)

U = 8.0, t’ = -0.20

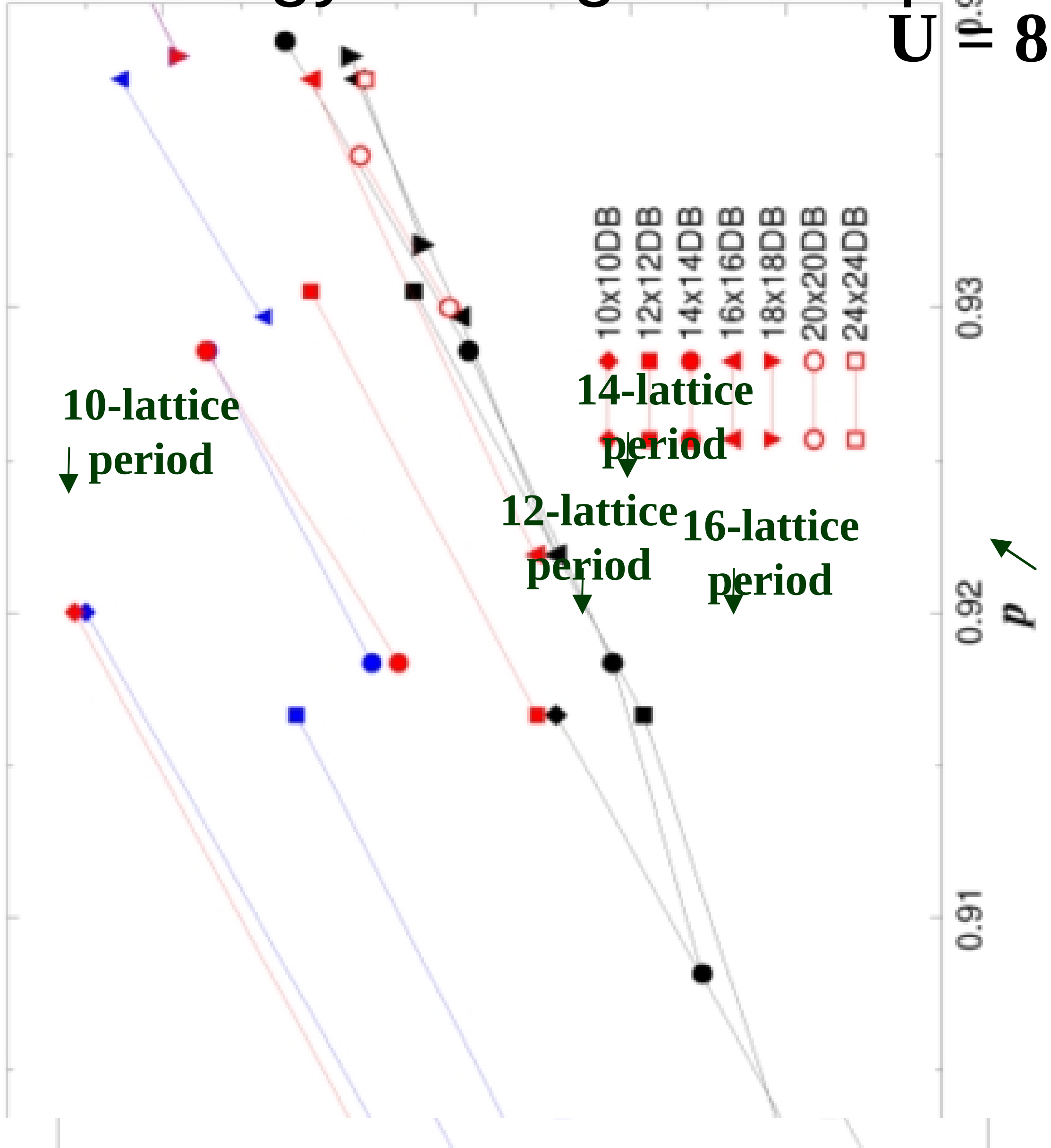

10-lattice period

12-lattice period

14-lattice period

16-lattice period

18-lattice period

20-lattice period

24-lattice period

Diagonal-stripe state can be stable In the lightly-doped region.

Total energy of striped states

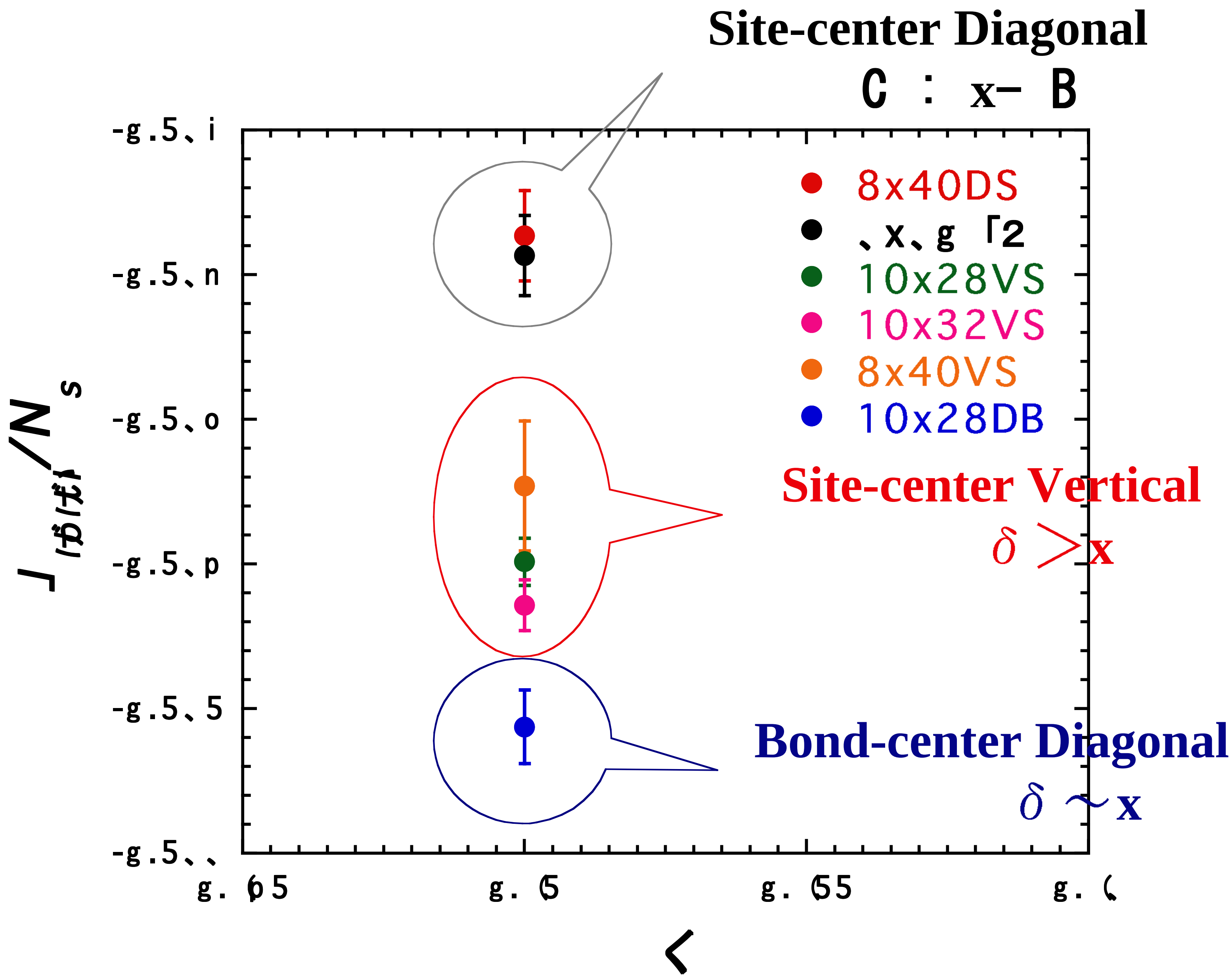

Incommensurability: Comparison with Experiments

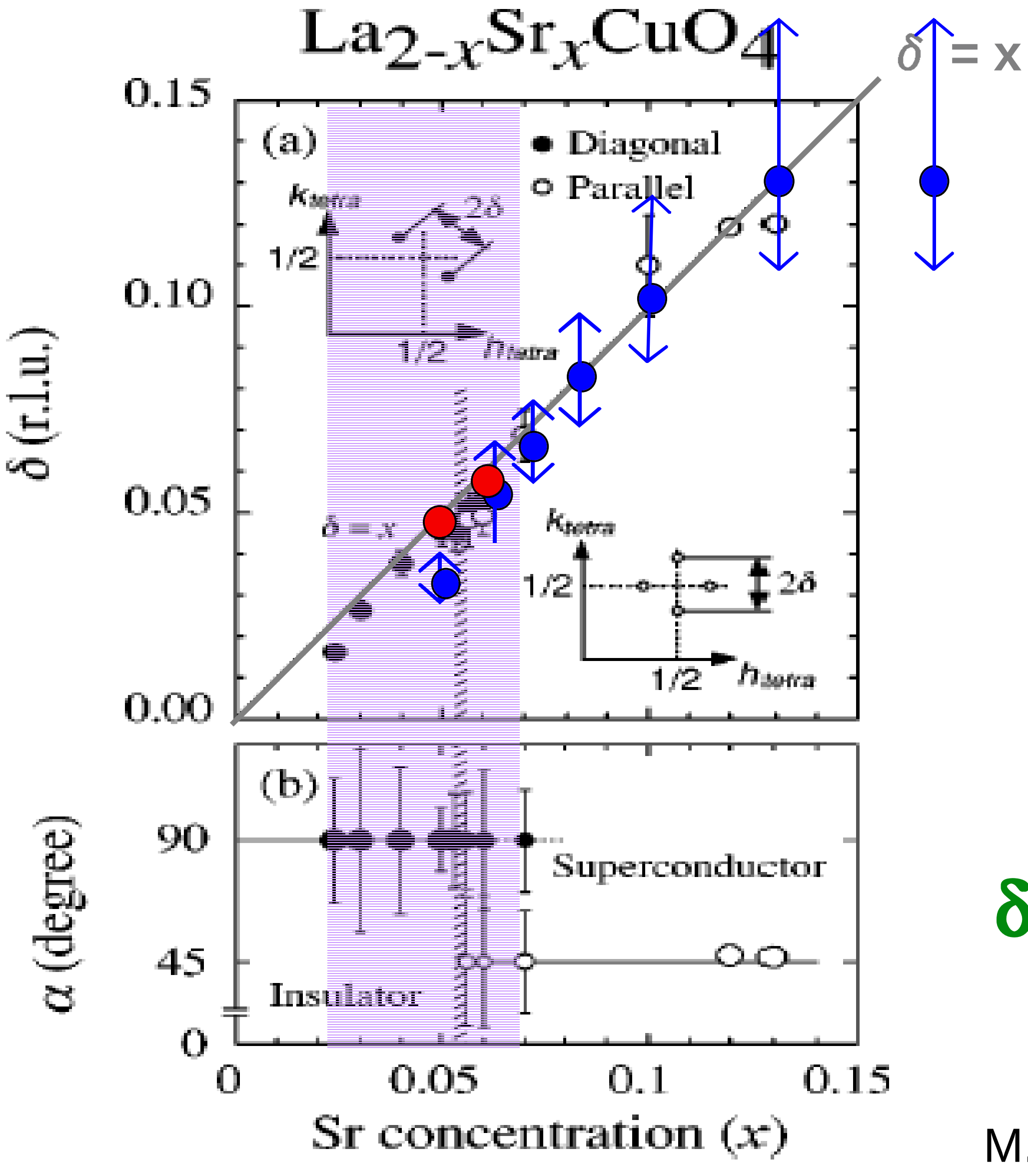

Vertical stripes

Diagonal stripes

U=8.0 t'= -0.2

δ can be explained by 2D Hubbard model.

M.Miyazaki et al., JPSJ 73(2004)1643.

8. Stripes and Structural transition

Structural transitions: Lattice distortions

LTT,LTO,LTLO,HTT

Stripes: suggested by Incommensurability

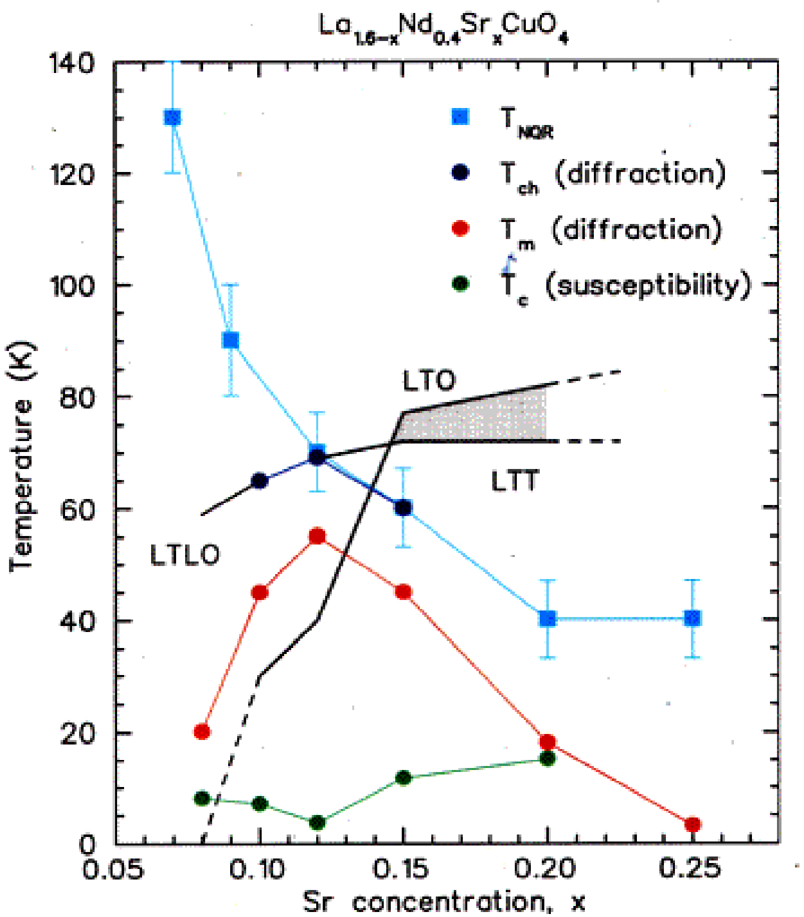

N.Ichikawa et al.
PRL85, 1738('00)

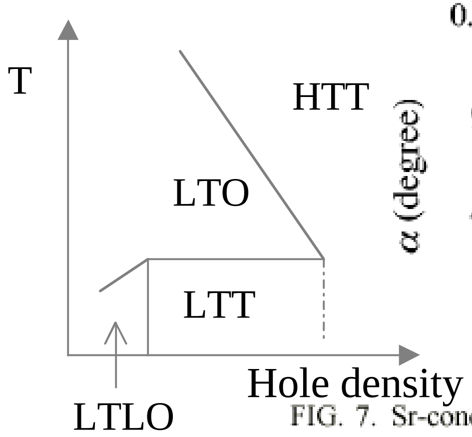

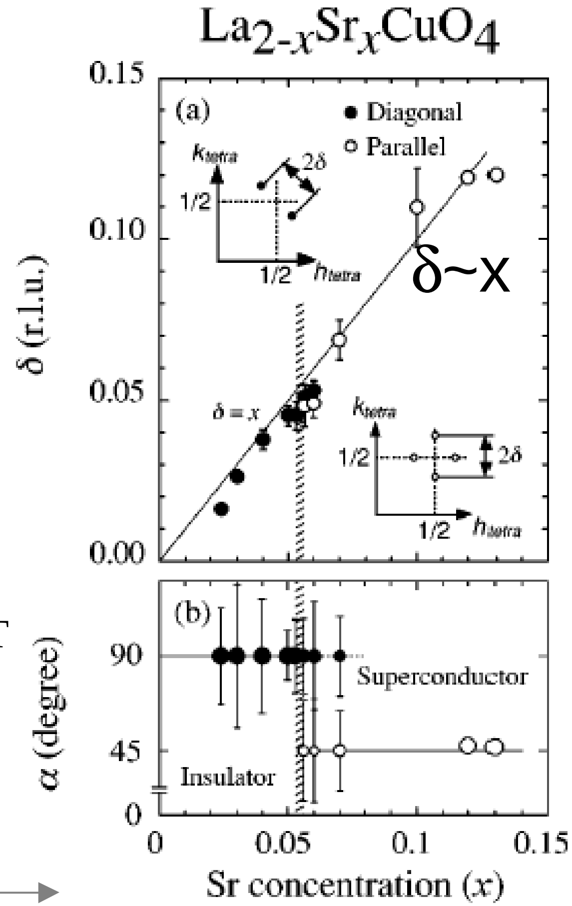

FIG. 7. Sr-concentration dependence of (a) the incommensurability δ and (b) the angle a defined in Fig. 3. Previous results for $x=0.024$ (Ref. 11), 0.04 (Ref. 10), 0.05 (Ref. 10), 0.12 (Ref. 5), 0.1 (Ref. 15), and 0.13 (Ref. 15) are included. In both figures, the solid and open symbols represent the results for the diagonal and parallel components, respectively.

M.Fujita et al. Phys. Rev.B65,064505('02)

What happens under lattice distortions?

1. Anisotropy of the transfer integrals
   Anisotropic electronic state
   vertical stripes
   Diagonal stripes x<0.05

2. Spin-Orbit Coupling induced from
   lattice distortions

3. Electron-phonon interaction

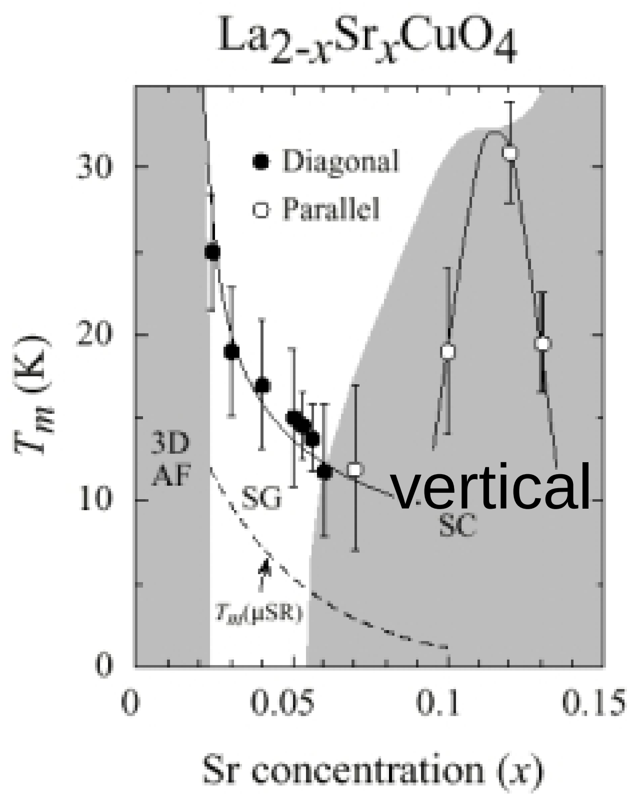

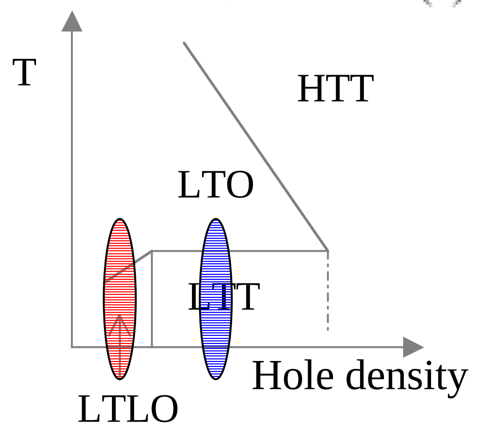

Anisotropy of the transfer integrals in LTT phase

Cf. A. P. Kampf et. al. PRB 64 (2001) 052509

One-band Hubbard model (Miyazaki)

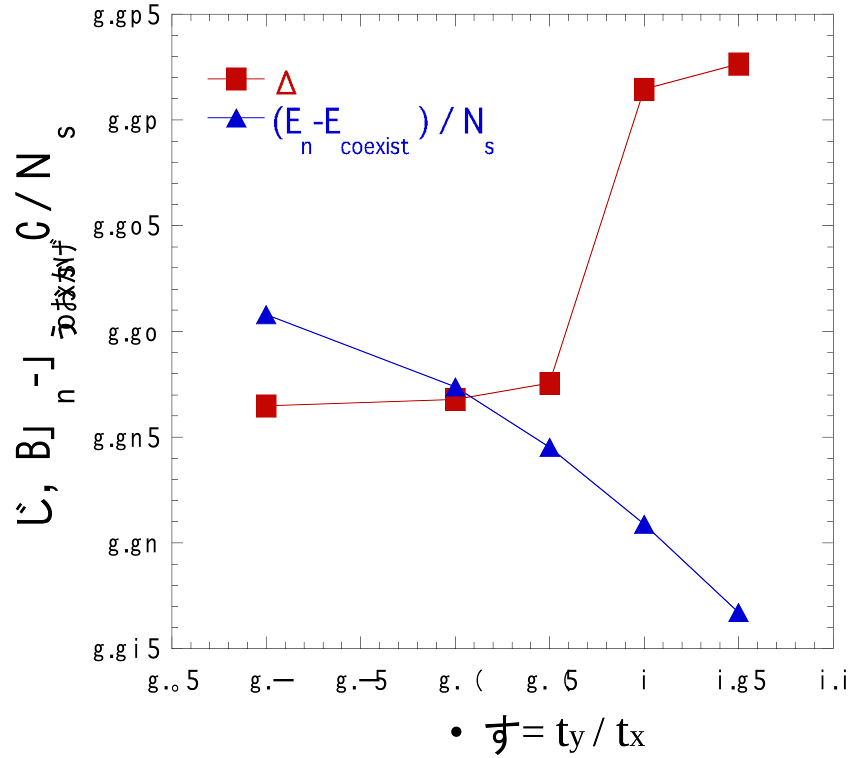

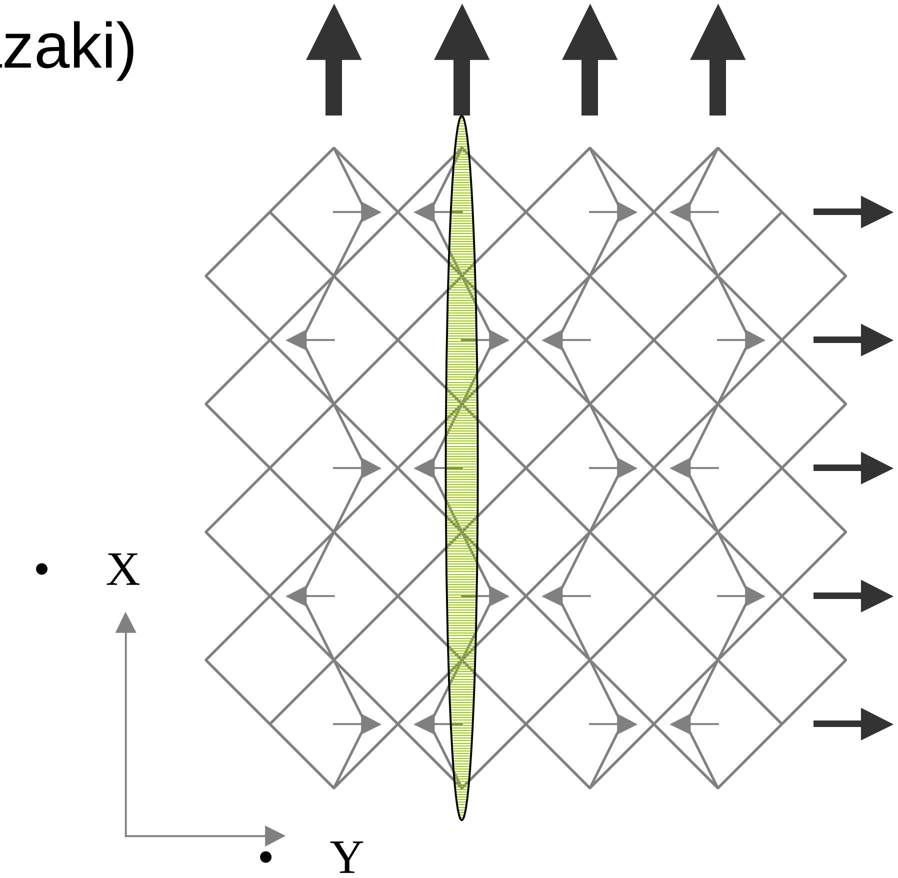

LTT structural transitions stabilize stripes.

Possible Stripe Structure 1

E. S. Bozin et. al. PRB 59 (1999) 4445
Lanzara et. al. J. Phys. Cond. Mat 11 (1999) 541

Mixed phase of LTT and LTLO

Stabilize stripes

M. K. Crawford et. al.

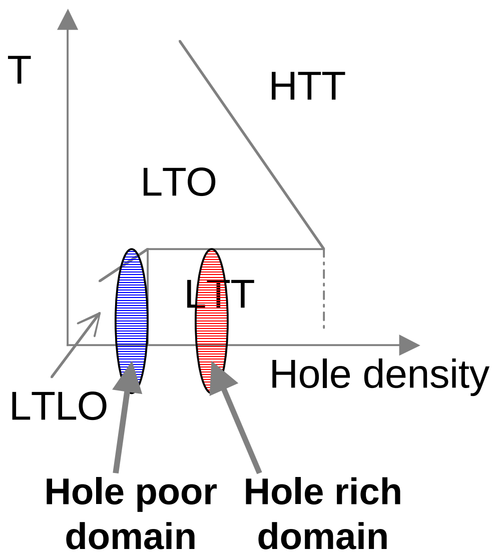

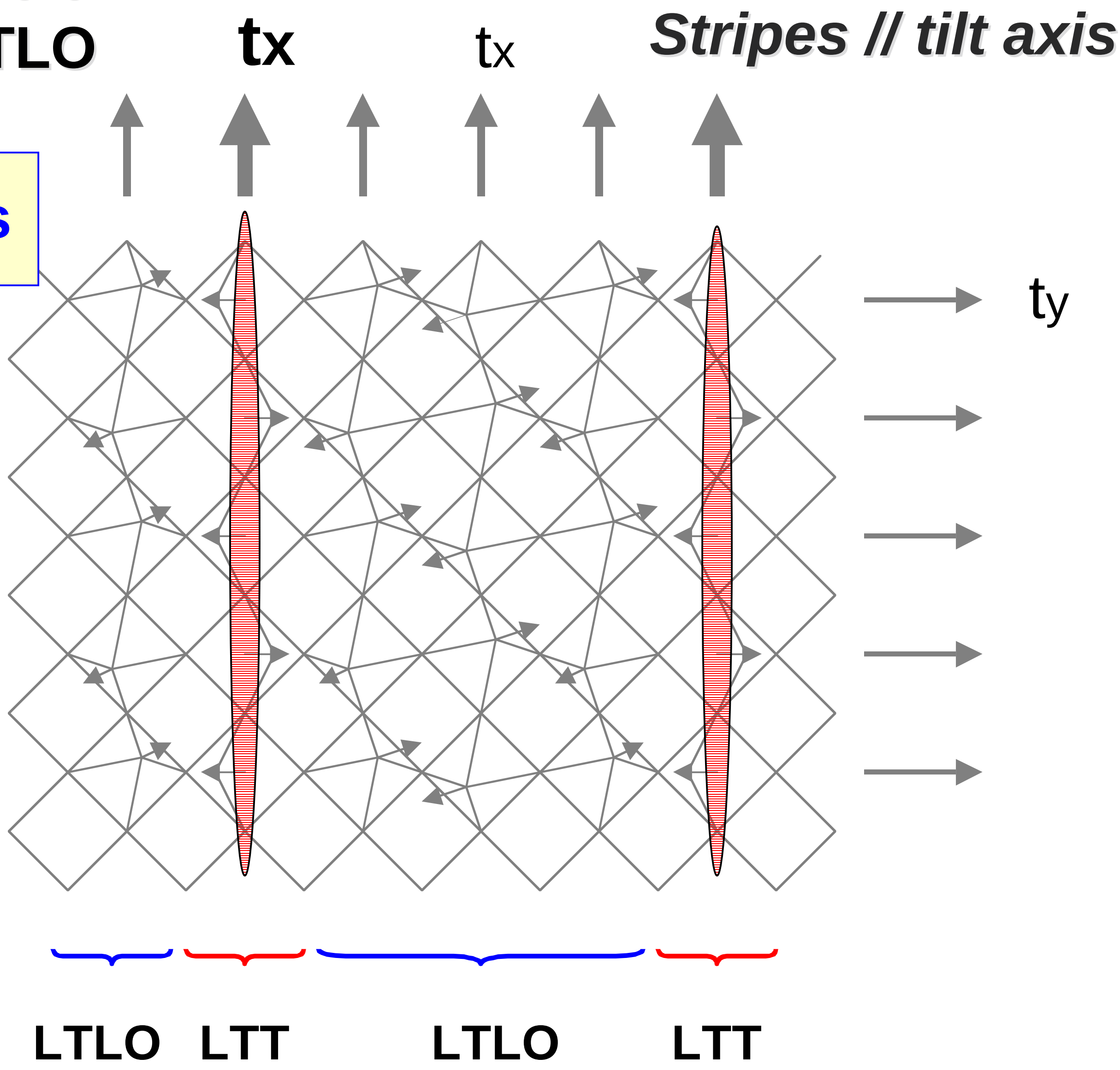

Possible Stripe Structure 2

Mixed phase of LTT and HTT

Stripes perpendicular to tilt axis

Stable

M. K. Crawford et. al.

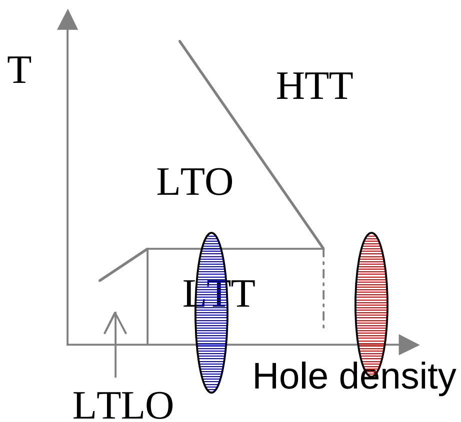

Oscillation of tilt angles

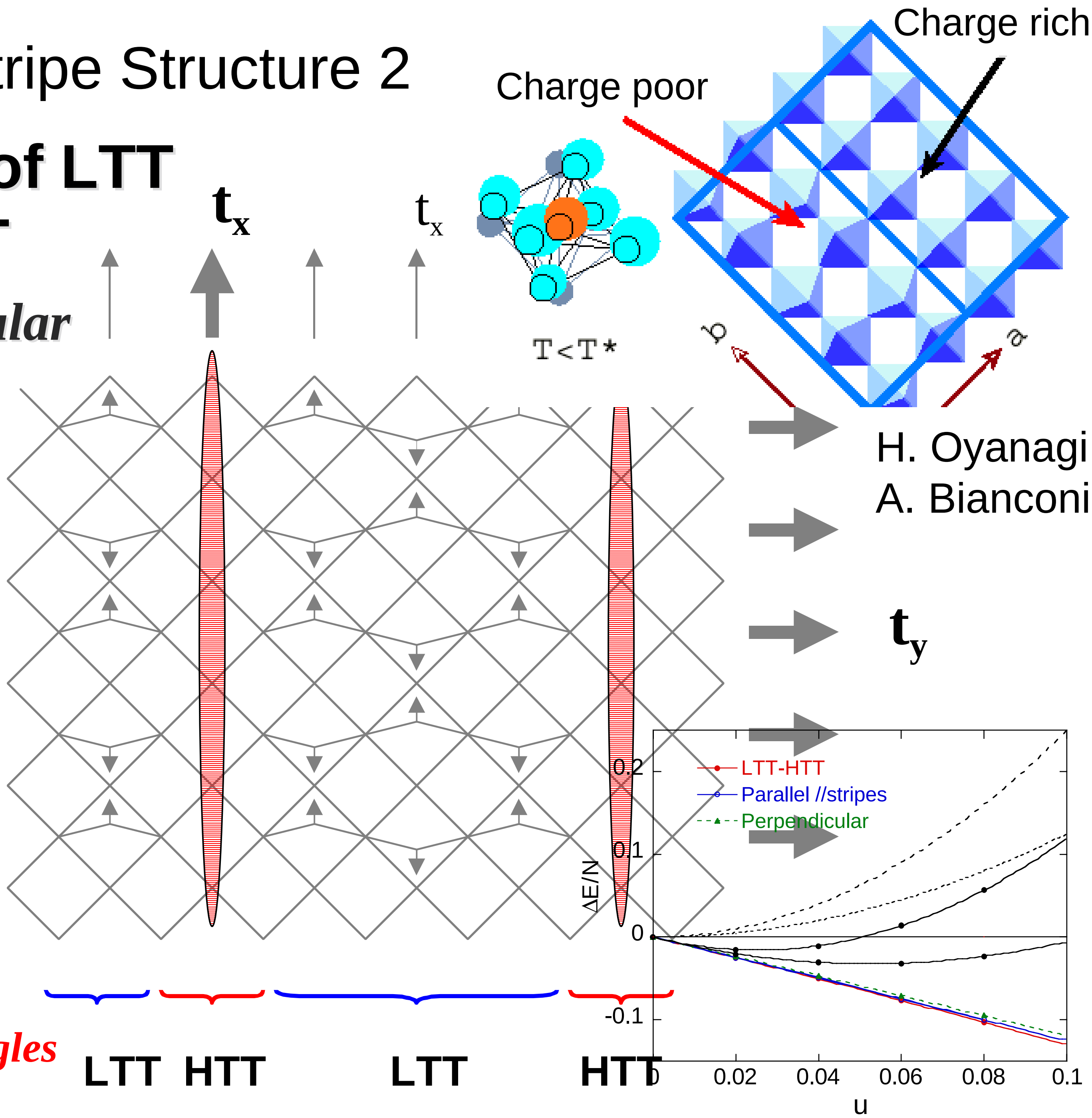

9. Spin-orbit coupling and Lattice distortion

Spin-Orbit Couling induced by the Lattice distortion

Friedel et al., J.Phys.Chem.Solids 25, 781 (1964)
K. Yamaji, J. Phys. Soc. Jpn. 57, 2745 (1988)

Tilting

$$\left\langle p_x(x-a/2,y)\uparrow\right|H_{dp}\left|d_{xz}(r)\uparrow\right\rangle = -t_{xz}e^{-ik_x/2\cdot a}$$

$$\left\langle p_y(x,y-a/2)\uparrow\right|H_{dp}\left|d_{yz}(r)\uparrow\right\rangle = -t_{yz}e^{-iky/2\cdot a}$$

$$H_{SO} = \xi(r)L\cdot S$$

$$\left\langle d_{xz}(r)\uparrow\right|H_{SO}\left|d_{yz}(r)\uparrow\right\rangle = -\frac{i}{2}\xi$$

$$\left\langle d_{yz}(r)\uparrow\right|H_{SO}\left|d_{xz}(r)\uparrow\right\rangle = \frac{i}{2}\xi$$

$$\left\langle d_{x^2-y^2}(r)\uparrow\right|H_{SO}\left|d_{yz}(r)\downarrow\right\rangle = \frac{i}{2}\xi$$

$$\left\langle d_{x^2-y^2}(r)\uparrow\right|H_{SO}\left|d_{xz}(r)\downarrow\right\rangle = \frac{1}{2}\xi$$

Effective iξ term for p-p transfer

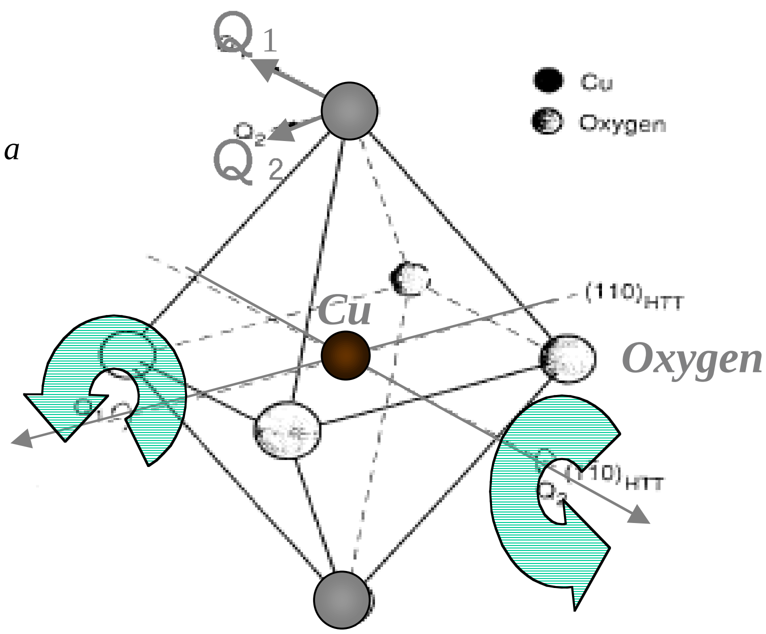

t_{xz}, t_{yz} ~ tilt angle

Five orbitals × (↑↓):
($d_{x^2-y^2}$, d_{xz}, d_{yz}, p_x, p_y)

Dispersion in the presence of spin-orbit coupling

d-p model

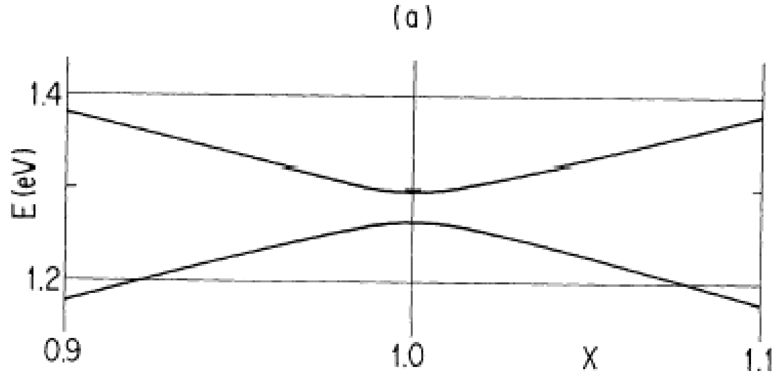

Zone boundary

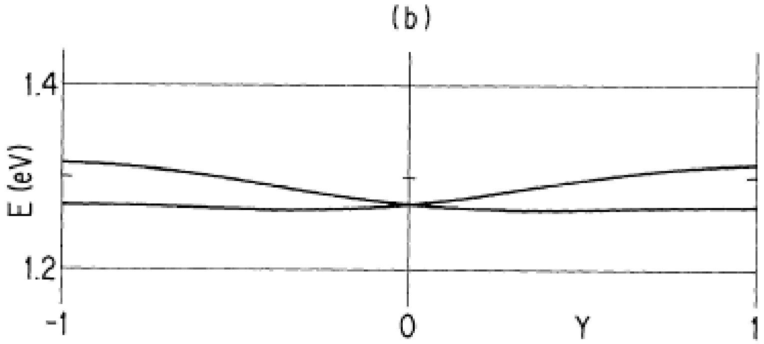

(π/2,π/2)

ξ = 0.4 (K.Yamaji, JPSJ(1988))

One-band effective model

$$H_{kin} = -\sum_{ij\sigma}(t_{ij} + ic\sigma\theta_{ij})d^{+}_{i\sigma}d_{j\sigma}$$

(Bonesteal et al.,PRL68,2684('92))

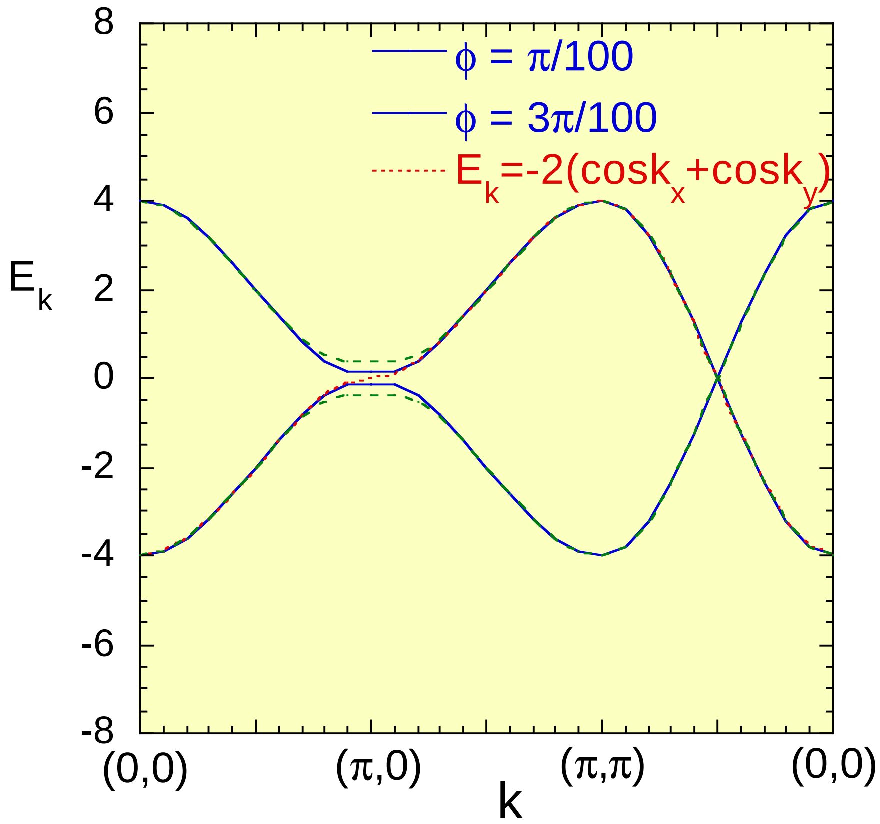

Flux state

$$E(k_x,k_y) = \pm\left| e^{i\phi/4}e^{ik_x} + e^{-i\phi/4}e^{ik_y} + e^{i\phi/4}e^{-ik_x} + e^{-i\phi/4}e^{-ik_y} \right|$$

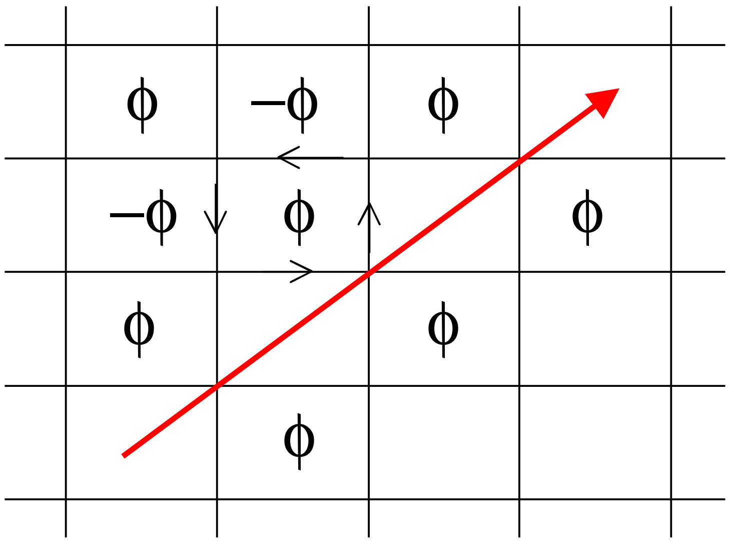

Excitation: Dirac fermion

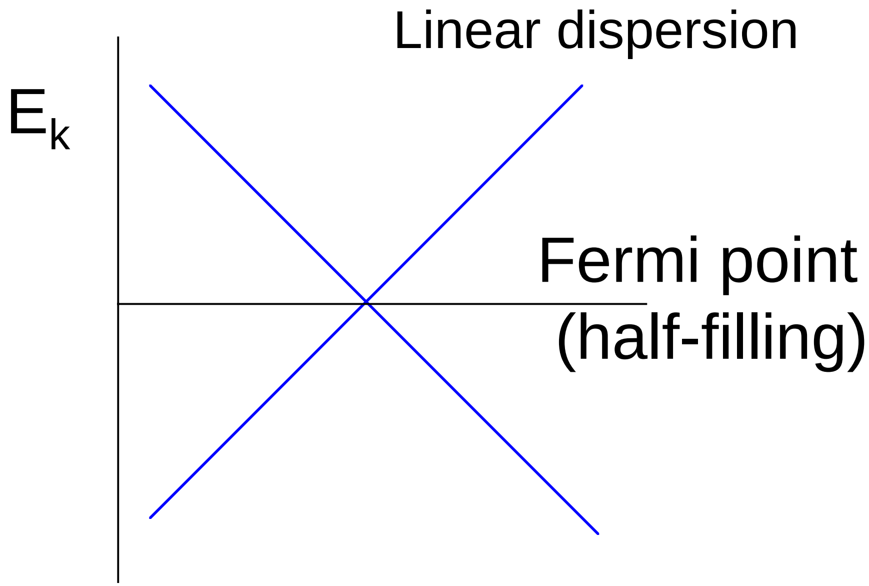

Small Fermi surface
Insulating or
Bad metal state

Stripe-density wave (inhomogeneous d-density wave)

Phenomena originating from spin-orbit coupling

Density of states

Pseudogap d $_{x2-y2}$ symmetry

Doping dependence of Spectral function

ARPES Fermi Arc

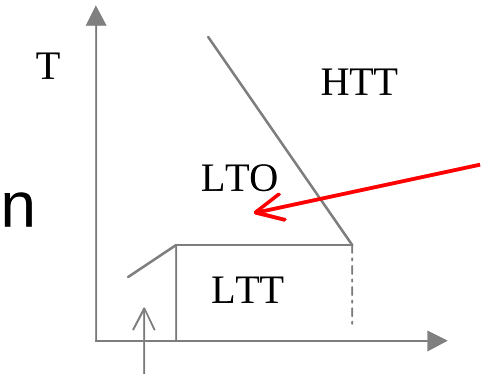

Nodal metal

Modification of the dispersion relation gap structure

Flux state d-density wave

Time reversal symmetry breaking

Stripes and spin-orbit

Stabilized diagonal stripes in the lightly-doped region

Generalization of d-density wave

Pseudo-gap in the density of states

Flux state

→ Pseudo-gap

An origin of pseudo-gap

Density of states

$$N_\sigma(k,\varepsilon) = -\frac{1}{\pi}\mathrm{Im}\,G_\sigma(k,\varepsilon+i\delta)$$

Eigenfunction $\varphi_{\sigma m}(r)$

$$H\varphi_{\sigma m}(r) = E_{\sigma m}\varphi_{\sigma m}(r)$$

$$G_\sigma(r,r',i\omega) = \sum_m \frac{\varphi_{\sigma m}(r)\varphi^*_{\sigma m}(r')}{i\omega - E_{\sigma m}}$$

T. Y. et al., JPSJ 74(2005)835.

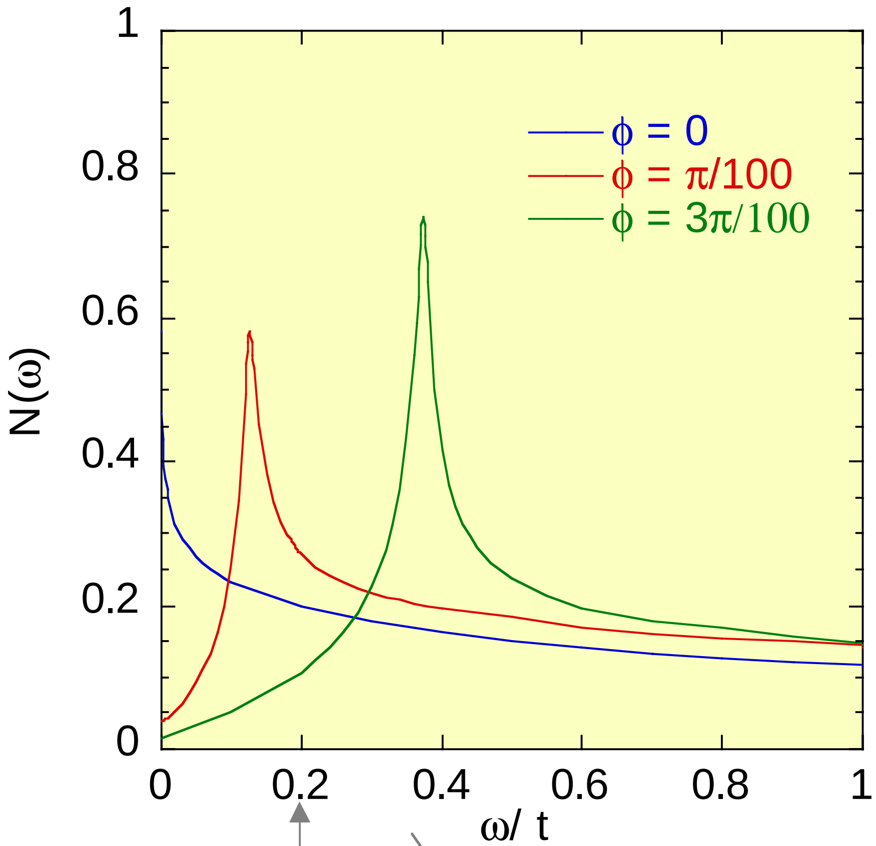

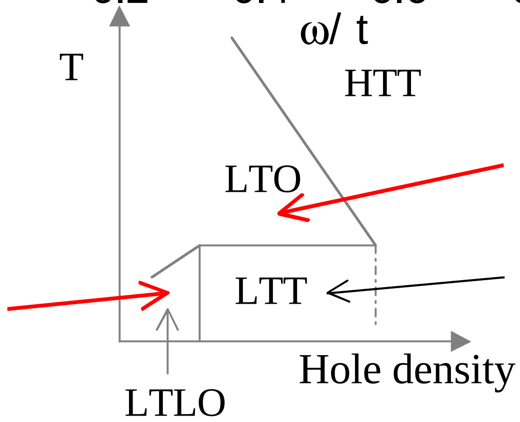

Diagonal stripes with Spin-orbit coupling

Diagonal stripes in Lightly doped region with Spin-orbit

Spin-orbit induces flux.

Spin-orbit coupling stabilizes the diagonal stripes.

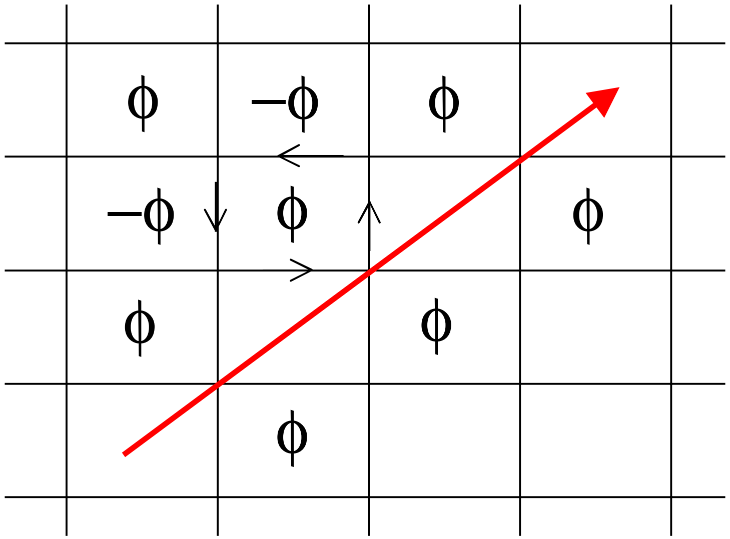

Diagonal Stripe & d-density wave

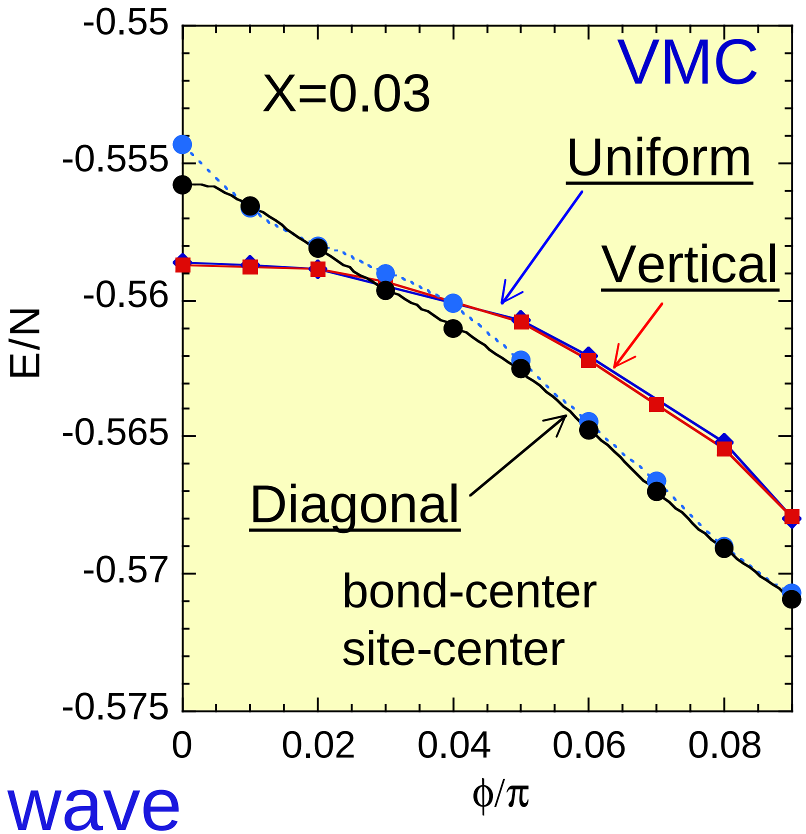

$\Phi = 4\phi$

d-density wave, string-density wave

d-density wave

$$i\Delta_Q Y(k) = \langle c^{+}_{k+Q\sigma} c_{k\sigma} \rangle \quad Q = (\pi, \pi)$$

$$Y(k) = \cos(k_x) - \cos(k_y)$$

Nayak, Phys. Rev. B62, 4880 (‘00)
Chakravarty et al., PRB63, 094503 (‘01)

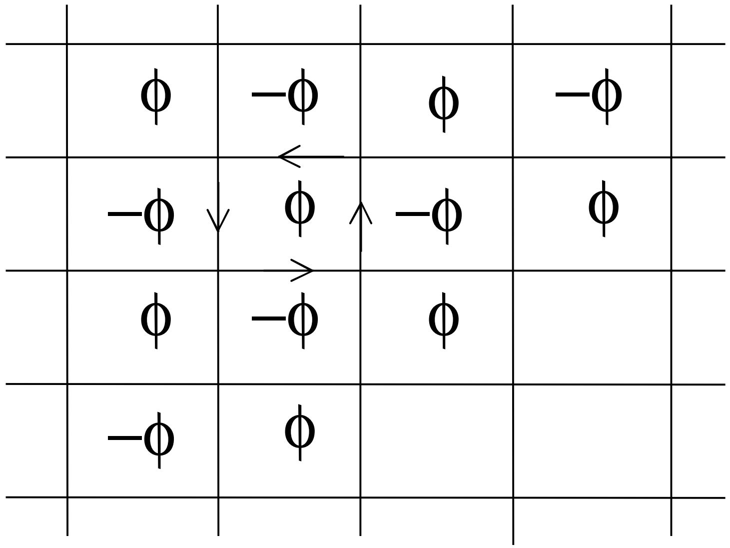

Incomm. density wave

Inhomogeneous density wave

$$i\Delta_Q Y(k) = \langle c^{+}_{k+Q\sigma} c_{k\sigma} \rangle$$ d-symmetry

$$\Delta_{lQ_s\sigma} = \sum_k \langle c^{+}_{k+lQ_s\sigma} c_{k\sigma} \rangle$$ incommensurate

$Q_s = (\pi+2\pi\delta, \pi)$ vertical

$Q_s = (\pi+2\pi\delta, \pi+2\pi\delta)$ diagonal

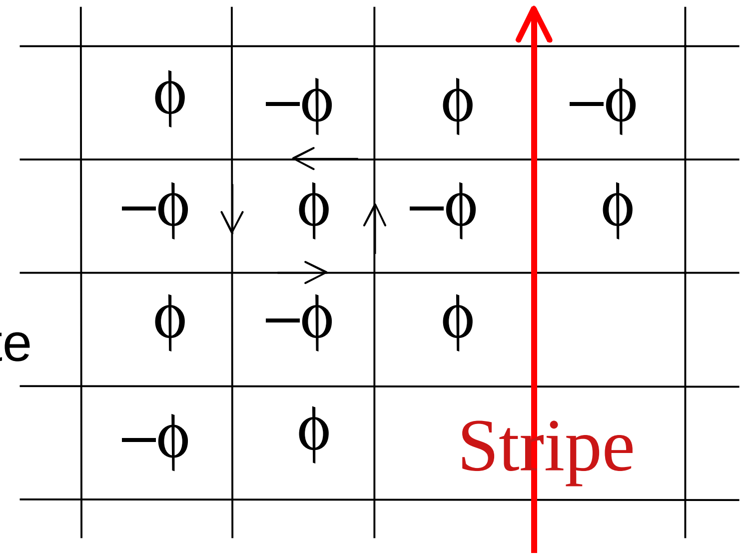

10. Spectra in the hole-doped cuprates
Fermi arc

Lightly doped region   x ~ 0.03

ARPES

Peak around (π/2,π/2)
(Cold spot in normal state

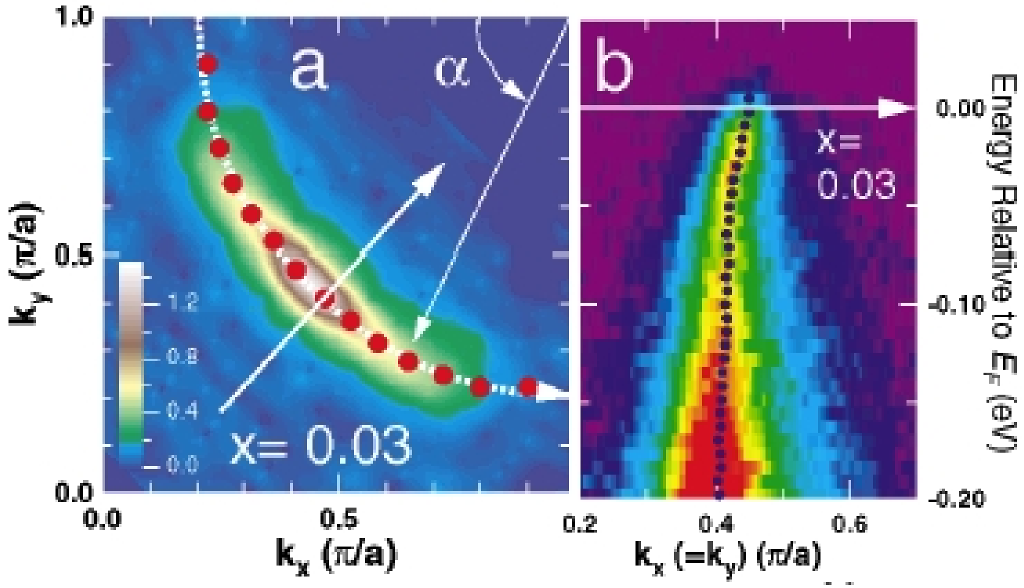

T.Yoshida et al. Phys. Rev. Lett. 91, 027001 (2003)

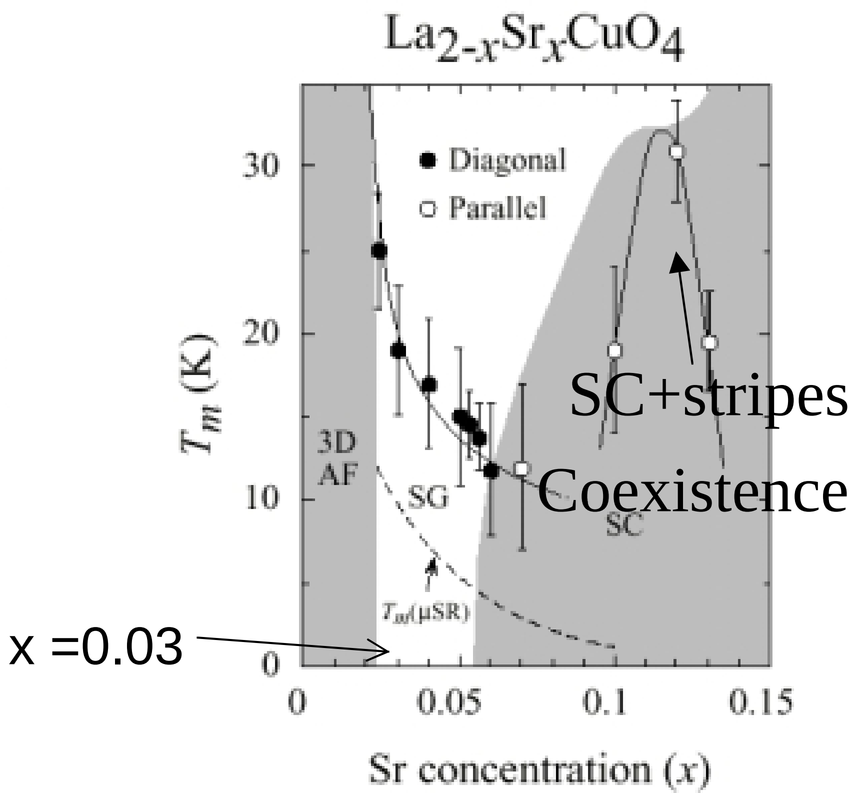

S.Wakimoto et al. PRB61, 3699('00)

A model for Arc-like Spectra
- Striped state and Tilted octahedron -

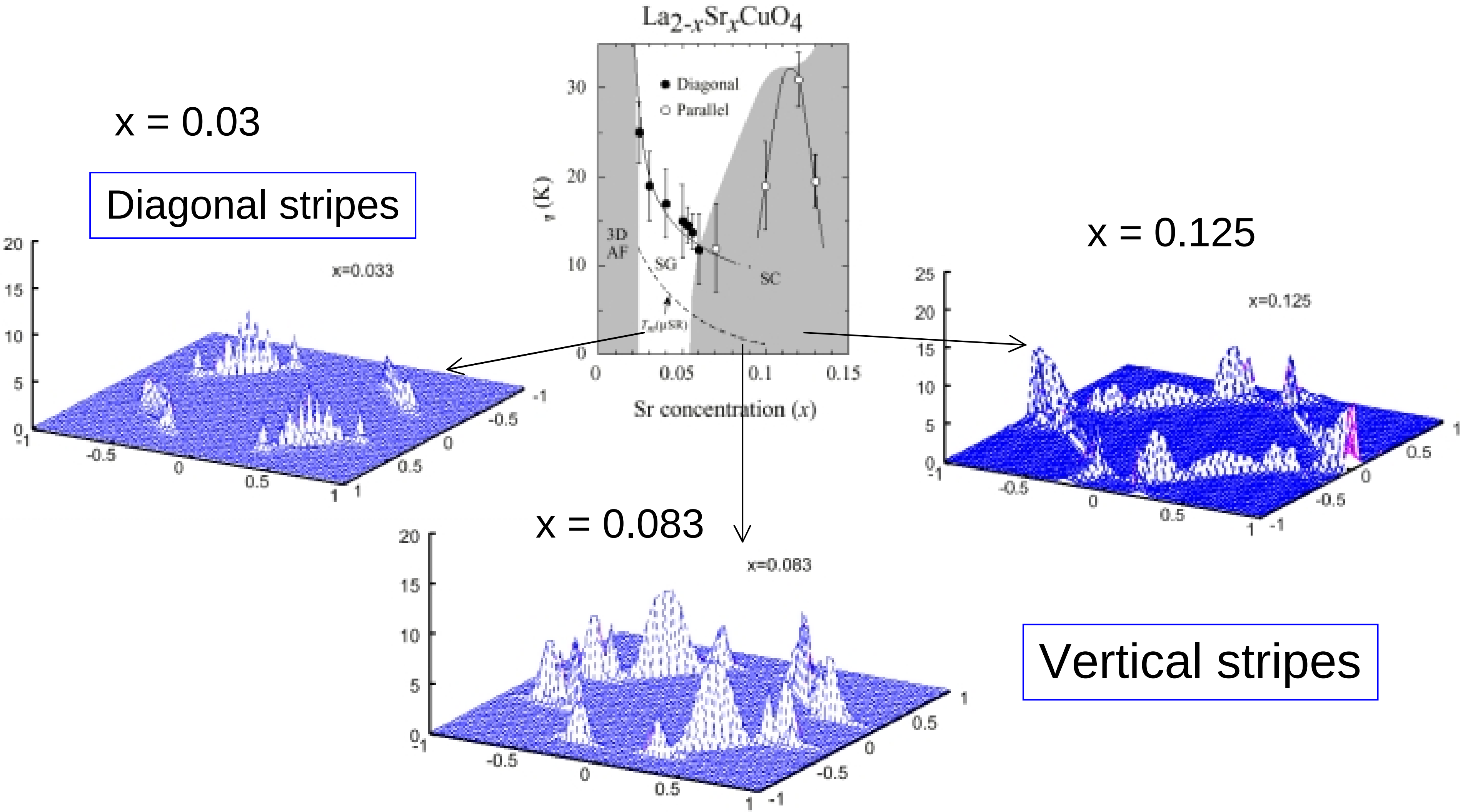

Flux state spectral function

ARPES

$(0,\pi)$

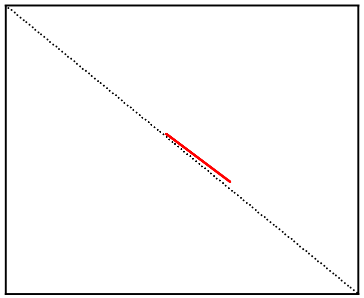

$(0,0)$ $(\pi,0)$

x= 0.028

Fermi arc

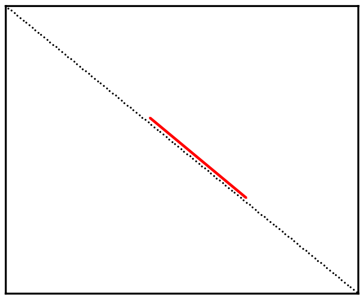

x= 0.072

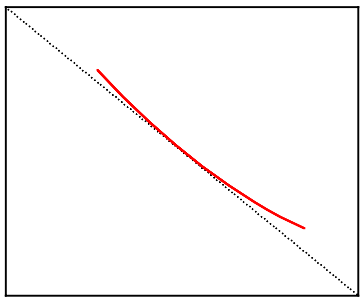

x= 0.13

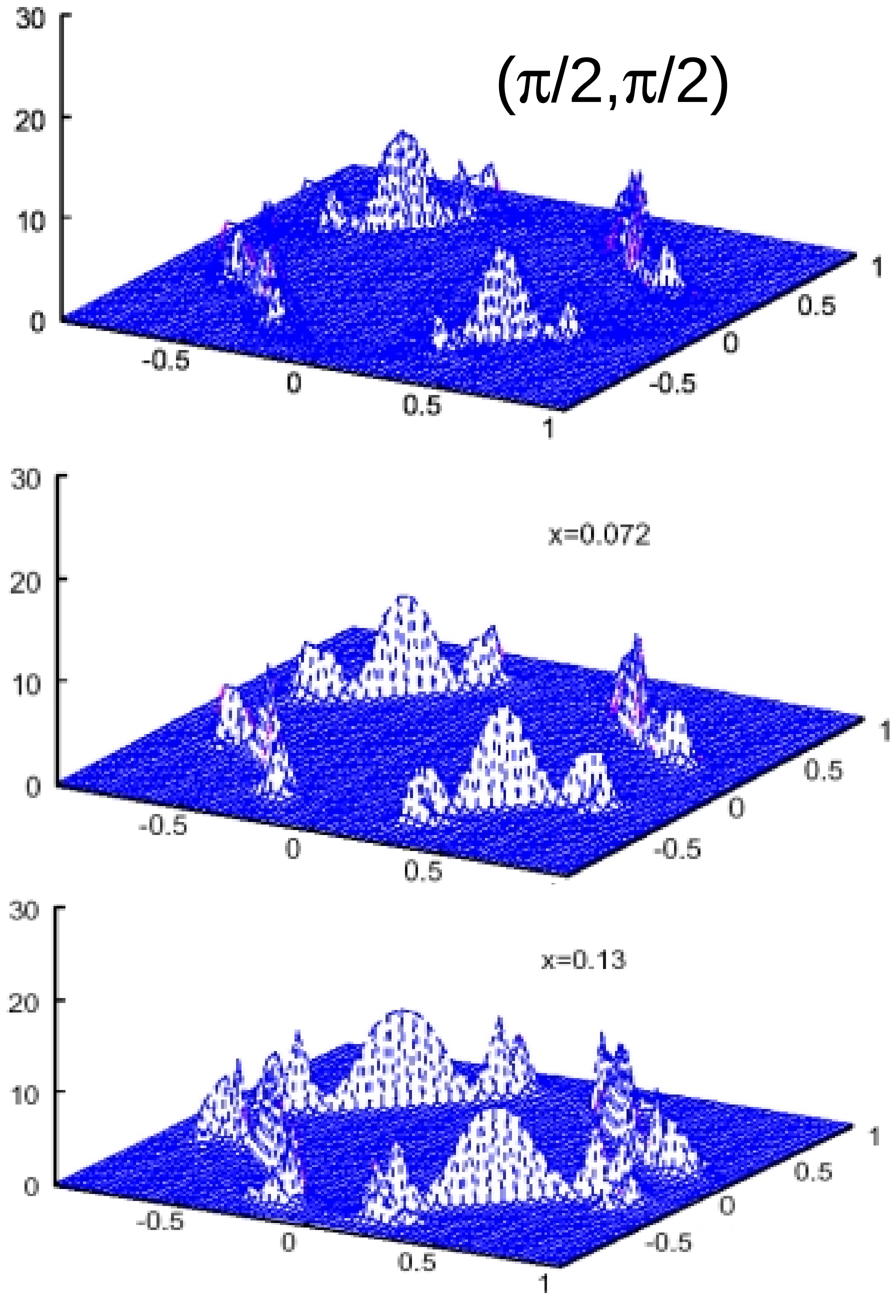

T. Y. et al, JPSJ 74(2005)835.

Spectra in the electron-doped region

$Nd_{2-x}Ce_xCuO_{4\pm\delta}$ [ARPES]

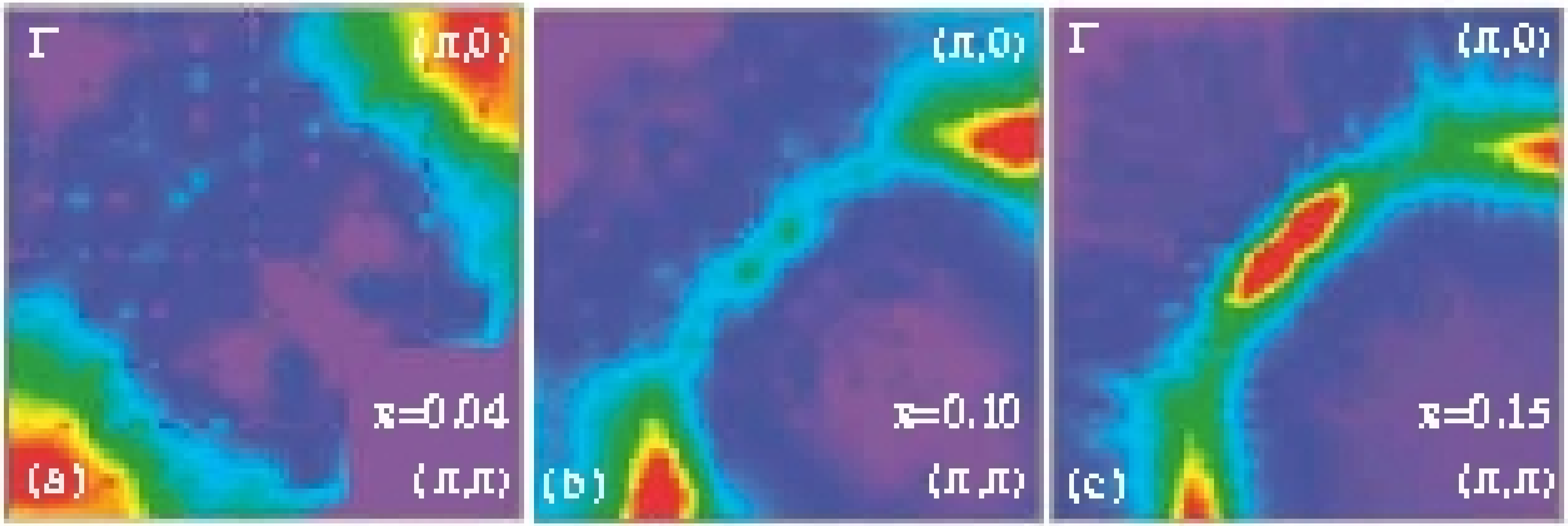

N. P. Armitage *et al.*, *Phys. Rev. Lett.* **88**(2002)257001.

11. Summary

1. SC in correlated electron systems

   = Gutzwiller-projected BCS

   LSCO t' small Bulk lmit of SC Condensation energy

   Bi2212 t',t'' AF correlation is weak due to FS.

   SC Cond. Energy is also small.

2. Vertical stripes : Compete and Coexist with SC
3. Diagonal stripes: Bond-center stripes for light doping
4. Spin-orbit and d-density wave

$\Delta E_{sc} \sim 0.2$ meV

(optimally doped)

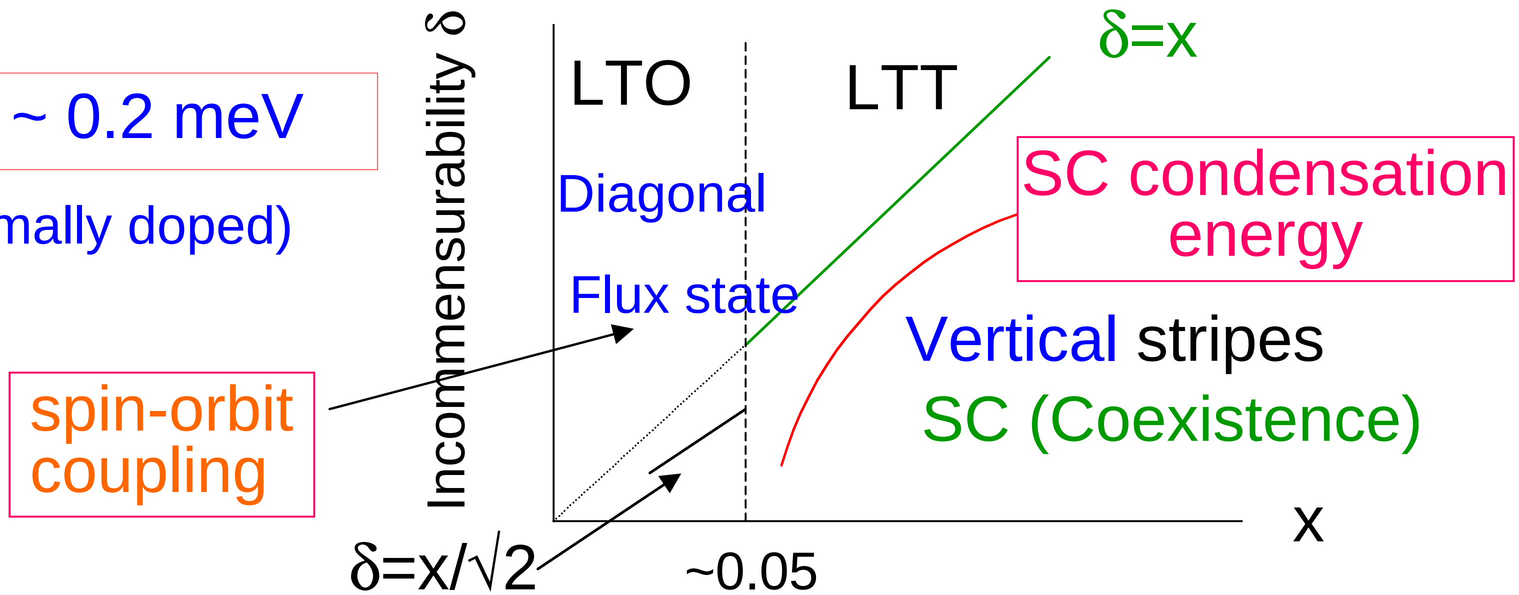

Summary of Theoretical study

Numerical calculations for the SC wave function

$$\psi_{CdS} = P_G \prod_k (u_k + v_k c^+_{k\uparrow} c^+_{-k\downarrow}) |0\rangle$$

Fermi arc spectra

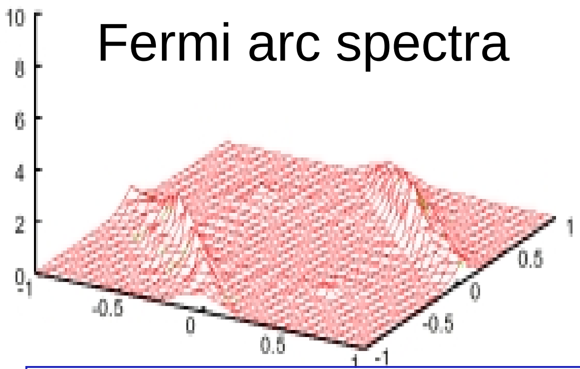

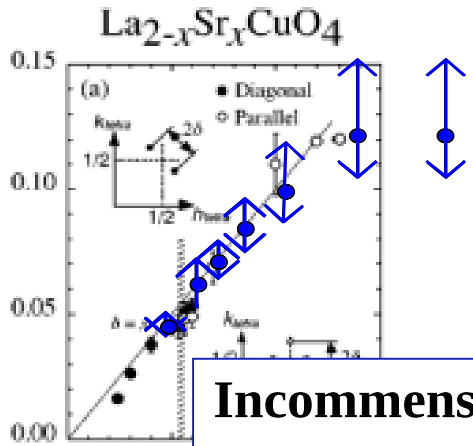

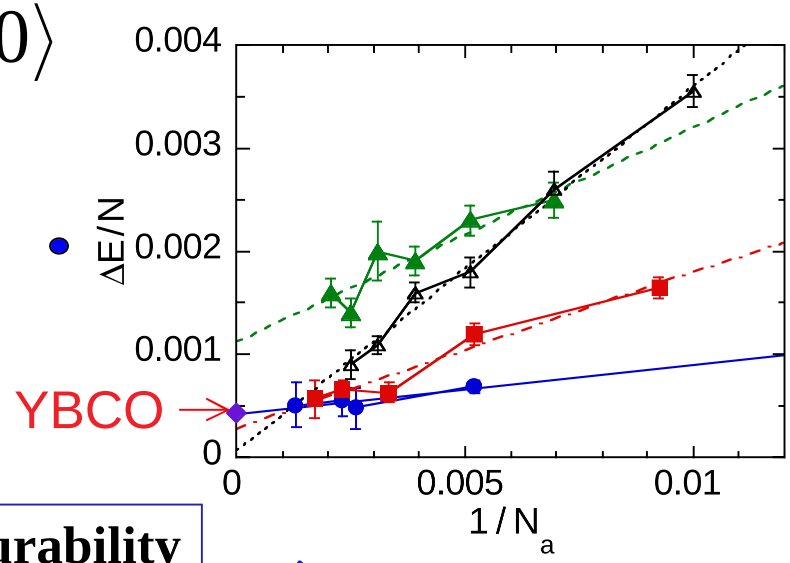

Incommensurability
Neutron scatterings

Explanation of spectra

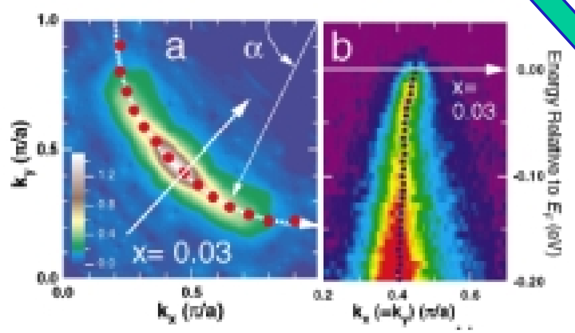

ARPES Measurements

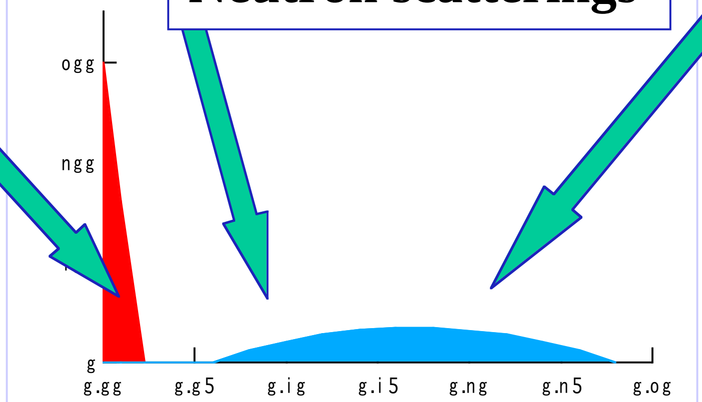

underdope

overdope

Theoretical estimate of SC condensation energy

Agreement with Exp.

E_{cond} ~ 0.2meV

Spare

Lattice Distortion

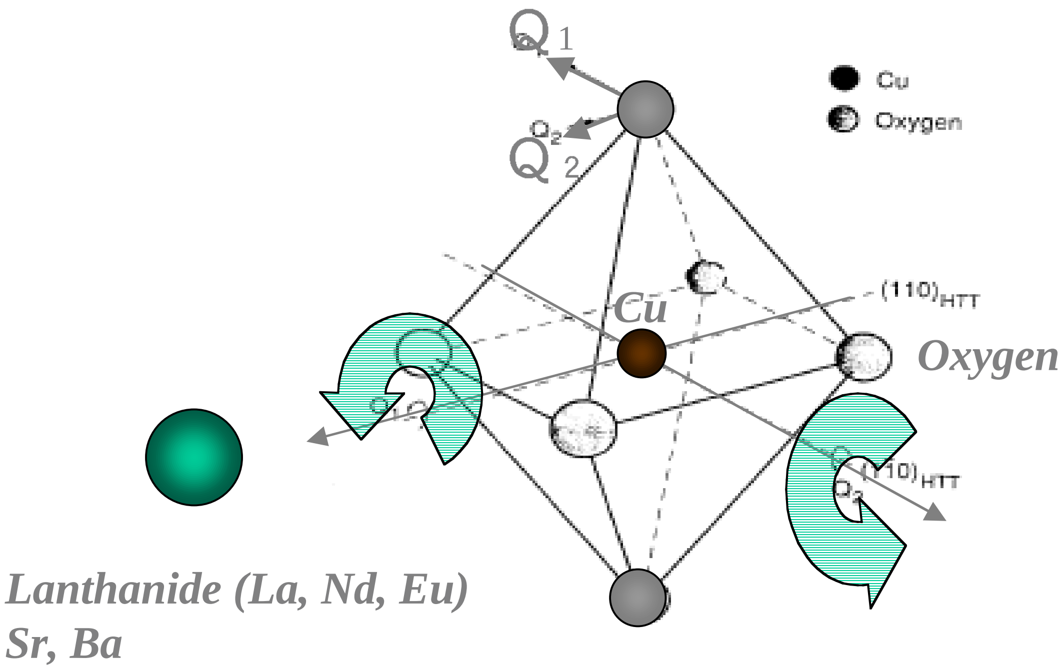

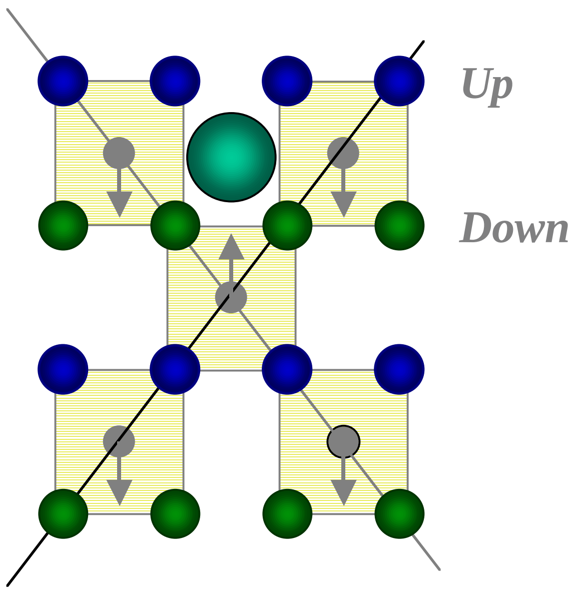

LTO (Q1=0,Q2 ≠0)
Almost isotropic

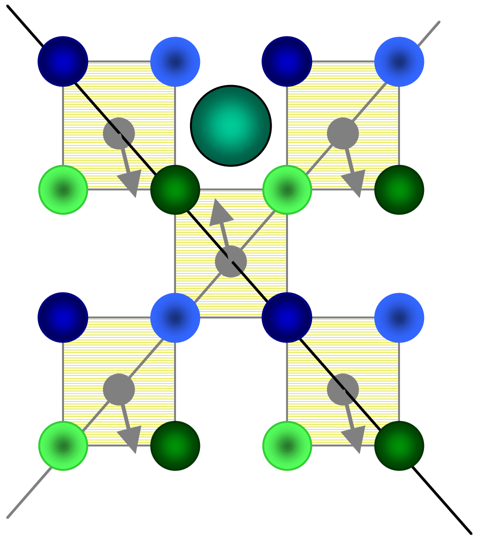

LTLO (Q1 ≠ Q2 ≠0)

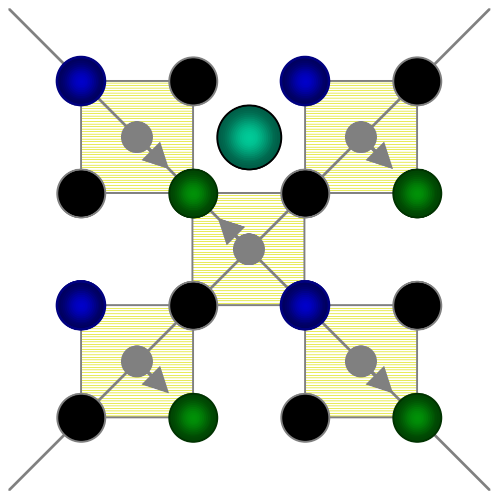

LTT (Q1= Q2 ≠0)
Anisotropic